Cite this: *J. Anal. At. Spectrom.*, 2011, **26**, 693

www.rsc.org/jaas

CRITICAL REVIEW

Inductively coupled plasma- and glow discharge plasma-sector field mass spectrometry†

Part I.‡ Tutorial: Fundamentals and instrumentation

Norbert Jakubowski,*[a] Thomas Prohaska,[b] Lothar Rottmann[c] and Frank Vanhaecke[d]

Received 17th September 2010, Accepted 23rd February 2011
DOI: 10.1039/c0ja00161a

The aim of this series of two reviews is to introduce the basic concepts of ICP and GD sector field instruments, to discuss their peculiarities and performance, to present selected analytical applications for demonstration of the 'state of the art' and, finally, to identify possible future trends and developments. Part I focuses on fundamentals, instrumentation and operation of instruments to give an overview of the capabilities of the actual commercially available instrumentation, whereas selected applications will be discussed in detail in part II.

[a]*BAM Federal Institute for Material Research and Testing, Richard-Willstaetter-Str. 11, D-12489 Berlin, Germany. E-mail: norbert.jakubowski@bam.de*
[b]*University of Natural Resources and Life Sciences (BOKU), Department of Chemistry, Division of Analytical Chemistry, (VIRIS Lab), Muthgasse 18, A-1190 Vienna, Austria. E-mail: thomas.prohaska@boku.ac.at*
[c]*Thermo Fisher Scientific, Hanna-Kunath-Str. 11, 28199 Bremen, Germany. E-mail: Lothar.Rottmann@thermofisher.com*
[d]*Department of Analytical Chemistry, Ghent University, Krijgslaan 281 – S12, B-9000 Ghent, Belgium. E-mail: frank.vanhaecke@UGent.be*

† This article is part of a themed issue highlighting the latest work in the area of Glow Discharge Spectroscopy, including work presented at the International Glow Discharge Spectroscopy Symposium 2010, August 22–25, Albi, France.

‡ For part II see ref. 182.

Norbert Jakubowski

Norbert Jakubowski has been Reviews Editor of JAAS since 2006. He studied physics at the University of Duisburg/Essen and completed his PhD in physics at the University of Hohenheim. He was a senior scientist at the Institute for Analytical Sciences, Dortmund and Berlin (from 1983 to 2009) and is now Head of BAM's Division I.1 Inorganic Chemical Analysis and Reference Materials (since July 2009). His research interests include inorganic trace and ultra-trace analysis of liquids and solids by use of ICP-MS and GD-MS, elemental speciation analysis and development of elemental tags for quantitative detection of biomolecules. He has received awards including the Alan Date Memorial Award from VG Elemental, Surrey, GB (1990), Zimmer International Scholar from University of Cincinnati, USA (2005) and a Waters Symposium Award for Pioneers in ICP-MS (2006).

Thomas Prohaska

Thomas Prohaska is professor for analytical chemistry at the University of Natural Resources and Life Sciences (BOKU). He studied Chemistry at the Vienna University of Technology, received his PhD with summa cum laude *in 1995 and became scientific researcher at the BOKU Vienna to built up a laboratory for elemental trace analysis. From 1998 to 2000 he was researcher at the EC-joint research center IRMM in Belgium. He returned to Vienna with a new focus on stable isotope research and became associate professor at the BOKU in 2002. In 2004 he received the START research award from the Austrian Science Fund (FWF) for the setup of a new isotope research laboratory (VIRIS).*

1 Introduction

This series of two reviews introduces in part I some basic concepts, operation principles and features and discusses the peculiarities and performance of commercially available instruments. Selected analytical applications will be discussed in part II to demonstrate the versatility of the devices described and some future trends will be pinpointed. Because more than 5000 articles related to sector field instruments for elemental analysis and more than 3000 related to isotopic analysis have been published up to now, it is only possible to discuss some selected examples in order to give an overview of the capabilities of this instrumentation. Additionally, this series of two papers will cover mainly the last 12 years, which is the period after the first reviews related to this topic were published.[1,2] A more comprehensive overview[3] or historic overviews[4,5] can be found elsewhere. It should be mentioned that this review does not cover all general aspects of inductively coupled plasma mass spectrometry (ICP-MS) and therefore, we recommend all those readers who are not familiar with ICP-MS at all to read the relevant books or book chapters first.[6–10]

Sector field instruments have a long and diverse history. Although we exclusively find sector field mass instruments in the early days of mass spectrometry, their importance declined and grew mainly related to their application in organic mass spectrometry, where high mass resolution was needed in particular for the analysis of complex samples. In parallel, sector field instruments have gained more and more relevance in inorganic mass spectrometry for quantitative elemental analysis and isotope ratio measurements. Different ionization devices such as, *e.g*, thermal ionisation (TIMS), electron impact (IRMS), secondary ionisation (SIMS) or the use of an ICP or glow discharge (GD) are found in the majority of today's inorganic mass spectrometers.

The goal of this tutorial is to discuss the main features, principles of operation and resulting applications of sector field mass spectrometers equipped with plasma (ICP or GD) sources. ICP and GD devices are discussed together since they show similar ionization properties of the analyte atoms in a plasma environment and use a similar mass spectrometer. Other devices are mentioned in some parts for comparison and are described in detail elsewhere.[11] Instrumental details will be described only for currently commercially available instrumentation.

A magnetic sector field can be used as a mass spectrometer in which ions are spatially separated as a function of their mass to charge ratio. Most often, the combination of a magnetic sector with an electric sector can be found in a variety of geometries. The electrostatic sector is used for focusing ions of different energies at an exit slit and thus the energy spread of the ions doesn't compromise the achievable mass resolution. Classic geometries include the Bainbridge–Jordan, Hinterberg–Konig, Takeshita, Matsuda, Mattauch–Herzog and Nier–Johnson geometries. The latter two geometries are used in commercial ICP and GD mass spectrometers and will be discussed later.

An important feature which accounts for much of the success of these devices is the capability to be operated at higher mass resolution (*i.e.*, greater than unity) in order to resolve interfering ions from the ions of interest. Thus, the instruments are most often applied whenever spectroscopic interferences become the limiting factor to the analytical performance. Even though high

Lothar Rottmann

Lothar Rottmann obtained his PhD in Analytical Chemistry in 1994 at the University of Regensburg under the supervision of Prof. Klaus Heumann. There, he developed a method for online isotope dilution of an HPLC/ICP-MS system. Afterwards he joined the R&D department of Thermo Fisher Scientific where he started as a research scientist. Since 1995 he has been a project manager, responsible for the development of several high resolution sector field instruments (Element 2, Element XR, and Element GD).

Frank Vanhaecke

Frank Vanhaecke obtained his PhD degree in 1992 from Ghent University (Belgium). He continued carrying out scientific research as a post-doctoral fellow at the same university and also enjoyed a post-doctoral stay at the Johannes Gutenberg University of Mainz (Germany). Since 1998, Frank Vanhaecke is Professor in Analytical Chemistry at Ghent University. His research interest is the determination, speciation and isotopic analysis of trace elements using ICP-MS. Special attention is devoted to the direct analysis of solid materials using both ETV-ICPMS and LA-ICPMS, chemical and high mass resolution for overcoming spectral interferences and isotope ratio determination using single- and multi-collector ICP-MS in the context of elemental assay via *isotope dilution, tracer experiments with stable isotopes and the use of small natural variations in the isotopic composition of metals and metalloids for unravelling geological and biological processes. He is (co-)author of some 150 journal papers and 300 conference presentations. In 2011, he received a European Plasma Award.*

Table 1 Commercial sector field mass spectrometer with plasma based ion sources 1985–2010

Name	Manufacturer[a]	Year of introduction	Status	Type of instrument	Geometry
VG 9000	VG Elemental	1985	discontinued	GD-SFMS	reverse Nier–Johnson
Plasmatrace I	VG Elemental	1988	discontinued	ICP-SFMS	Nier–Johnson
JMS-Plasmax 1	JEOL	1991	discontinued	ICP-SFMS	reverse Nier–Johnson
Plasma 54	VG Elemental	1992	discontinued	MC-ICP-SFMS	Nier–Johnson
Element	Finnigan MAT	1993	discontinued	ICP-SFMS	reverse Nier–Johnson
Plasmatrace II	VG Elemental	1994	discontinued	ICP-SFMS	reverse Nier–Johnson
JMS-Plasmax 2	JEOL	1995	discontinued	ICP-SFMS	reverse Nier–Johnson
Nu Plasma	Nu Instruments	1997	discontinued	MC-ICP-SFMS	Nier–Johnson
Axiom	VG Elemental	1998	discontinued	ICP-SFMS	Nier–Johnson
Axiom MC	VG Elemental	1998	discontinued	MC-ICP-SFMS	Nier–Johnson
Element 2	Thermo Quest	1998	available	ICP-SFMS	reverse Nier–Johnson
Nu Plasma 1700	Nu Instruments	1999	available	MC-ICP-SFMS	Nier–Johnson
Neptune	Thermo Quest	2000	available	MC-ICP-SFMS	Nier–Johnson
IsoProbe-P	GV Instruments	2004	discontinued	MC-ICP-SFMS	magnetic sector + hexapole collision cell
Element XR	Thermo Electron	2004	available	ICP-SFMS	reverse Nier–Johnson
AttoM	Nu Instruments	2004	available	ICP-SFMS	Nier–Johnson
Element GD	Thermo Electron	2005	available	GD-SFMS	reverse Nier–Johnson
SPECTRO MS	Spectro Analytical Instruments	2010	available	MC-ICP-SFMS	Mattauch–Herzog
Nu Plasma II	Nu Instruments	2010	available	MC-ICP-SFMS	Nier–Johnson
Astrum	Nu Instruments	2010	available	GD-SFMS	Nier–Johnson
Neptune plus	Thermo Scientific	2009	available	MC-ICP-SFMS	Nier–Johnson

[a] Manufacturer names are according to their names when the instrument was introduced.

sensitivity and high mass resolution capabilities are the most prominent specific characteristics, magnetic sector field instruments offer another unique feature which is difficult or impossible to achieve with other mass separators (*e.g.*, quadrupole based instruments): real simultaneous detection of ions, which is the raison dêtre for instruments with multiple collectors. More details on isotope ratio measurements are found in a comprehensive overview[12] and an additional tutorial.[13]

Therefore, inorganic sector field devices can be grouped in two categories depending on their intended use: The first category comprises instruments which are used in scanning mode for multi-element analysis. These instruments are usually equipped with one detector (electron multiplier) and can also have an additional Faraday cup in order to extend the linear dynamic detection range. Therefore, the intensity of the ion beam of one particular nuclide is monitored at a time. These instruments are called single collector ICP-SFMS and are mostly referred to just as ICP-SFMS. In some occasions, the abbreviation HR-ICP-MS can be found, which refers to single collector ICP-SFMS instruments operated in high mass resolution.

The second category of instruments is usually operated in static mode in order to detect multiple ion beams simultaneously on a set of detectors (faraday cups and/or multiple ion counters or on channel plate-type array detectors). This type of instrument is called multiple collector ICP-SFMS (MC-ICP-SFMS). In literature, the abbreviation MC-ICP-MS is commonly used as it is expected to be clear that the mass separator of this instrument is a magnetic sector field. The main application of these instruments is isotope ratio measurements.

The following acronyms will be used throughout this paper, irrespective of whether or not these are in agreement with other literature: ICP-MS is used whenever general aspects of the method are concerned. ICP-QMS is used whenever the mass analyser in question is a low resolution quadrupole filter. ICP-SFMS is used whenever an instrument with sector fields is applied. As said before, the latter instruments can be operated at low mass resolution ($m/\Delta m$ = 300–400) or at higher mass resolution ($m/\Delta m$ > 1000). Multi-collector instruments are indicated as MC-ICP-SFMS.

During the last 15 years, 20 commercially available instruments were introduced to the market (Table 1). Historically, the *VG 9000* GDMS[14] was the first commercially available double focusing instrument used for elemental analysis. This instrument had a glow discharge plasma ion source and was introduced in 1985. In 1988, VG introduced the *Plasmatrace*, the first single collector inductively coupled plasma sector field instrument.[15,16] While the response from the analytical community fulfilled the expectation of the manufacturer for the *VG 9000*, the acceptance of the *Plasmatrace* by the analytical community was far more hesitant. This was mainly due to its complexity (relative to quadrupole ICP-MS) and the consequently high sales price. The situation changed significantly when a more user-friendly second generation of a technically improved new instrument was made available at a much lower price about five years later.[17] The instruments found their way into applied science and routine analysis as limitations caused by spectral interferences became more widely realized, along with a steadily increasing demand for improved accuracy and lower limits of detection in many areas of geological, environmental, medical and biological research.

By 2010, about 700 single collector, about 250 multi-collector ICP-SFMS and about 125 GD-SFMS have been sold. The major reasons for the success can be summarized as follows (data from ref. 18):

- the higher sensitivity (slope of the calibration graph) at a resolution comparable to quadrupole-based instruments,

• the low instrumental background (most often below 1 count per second),

• the lower limits of detection (the higher sensitivity, lower background and high mass resolution contribute to the lower limits of detection, which most often are only limited by the blanks of the chemicals and working tools used for analysis),

• the capability to separate the majority of chemically different ions contributing to a signal at the same nominal *m*/*z* ratio as the ion of interest (spectral interferences) by applying high mass resolution,

• the capability of an accurate mass determination at high mass resolution, by which, for instance, an interfering species can be identified,

• higher precision due to the capability of simultaneous measurement of ions of different *m*/*z* ratio (isotope ratios).

2 History

The long and splendid history of sector field instruments started more than 100 years ago. They were used in the early days of mass spectrometry by Joseph J. Thomson, who received the Nobel Prize in Physics for the discovery of the electron in 1906 even though the roots of sector fields go back much further (Fig. 1). In 1886, the German physicist Eugen Goldstein, who studied under Hermann von Helmholtz, coined the term 'cathode rays' for the negatively-charged electrons discovered by Johann Hittorf, which are emitted when electric current is forced through a vacuum tube. He also discovered 'Kanalstrahlen' (canal rays), positively-charged particles formed when electrons are removed from gas particles in a glass tube filled with gas at reduced pressure and equipped with a perforated cathode. In 1898, Wilhelm Wien demonstrated that these canal rays could be deflected by a strong superimposed electric and magnetic sector field.

J. J. Thomson[19] started his studies of the 'Kanalstrahlen' in 1905 and he improved the blurred parabolas obtained by Wien by reducing the pressure in his apparatus. Thus, he was able to obtain sharp parabolas for H^+ and H_2^+. Later, he used a metal plate in which a parabolic slit was cut. By varying the magnetic field strength and measuring the current of the ion beam that passed through the slit, he was able to plot the ion current *versus* mass. He used his device to determine the isotopic composition of stable elements (for instance neon) together with his student, Francis Aston. The latter received the Nobel Prize in chemistry in 1922. In 1919, Aston[20] significantly improved the first mass spectrometer by separating electric and magnetic fields and arranging them in a way that all ions are focused in a plane of a photo plate. At that time, he achieved a resolution of about 130. Of the 283 nuclides of the 83 elements known in 1948, 202 nuclides of 71 elements were found by Aston. While Thomson was the father of mass spectrometry, Aston is definitely the father of isotopes. He was the first who used the term 'mass spectrum' in 1920.

In 1929, Arthur J. Dempster (and Bartky) designed and built a spectrometer with a 180° magnetic sector geometry with directional and velocity focusing. Later, he combined the instruments with new ion sources, such as an electron impact source or spark source in 1934. In 1935, Dempster[21] developed the first 'scanning' mass spectrometer. In this device, the separation of ions focused into an exit slit was already related directly to the *m*/*z* ratio. Scanning was performed either by changing the magnetic field or the acceleration voltage. He applied a Faraday detector and electronic amplification for detection of the ions. Later, he used his electron impact source for ion generation in molecular mass spectrometry as well, resulting in the first molecular mass spectrum. He is also famous for the development of a radio frequency spark source (in 1934), a discharge generating a discontinuous short-term plasma, for direct generation of

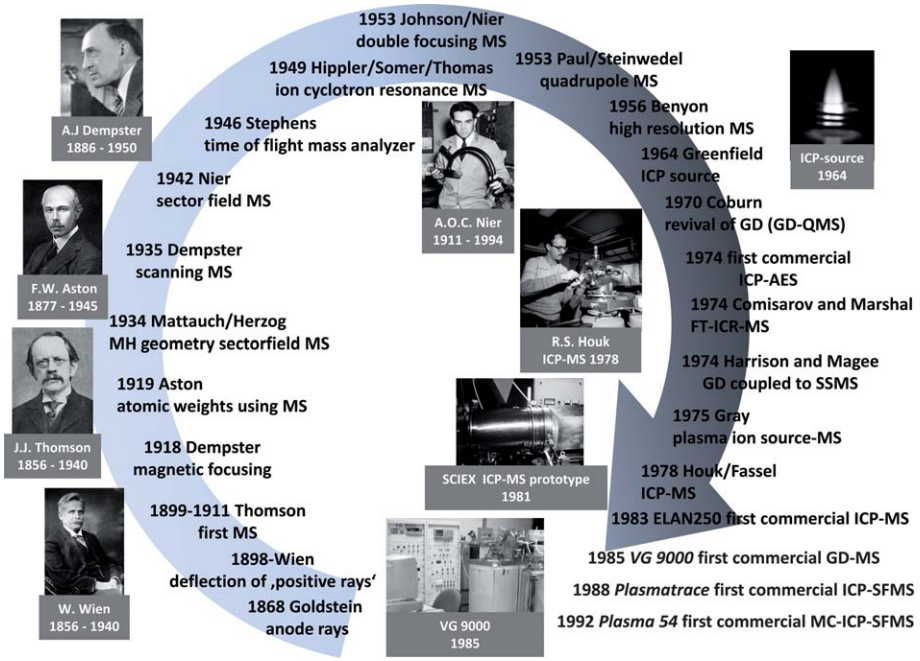

Fig. 1 History of mass spectrometry – highlights and developments.

ions from conducting materials, such as metals.[22] Dempster's research led to the discovery of the uranium isotope ^{235}U in 1935.

Many scientists have been involved in the further development of instruments with directional and velocity focusing. The team of Mattauch and Herzog should be noted, as they have contributed significantly to the development of double-focusing instruments in 1934 with the well known Mattauch–Herzog geometry – consisting of a 31.8° ($\pi/4\sqrt{2}$) electric sector field and a 90° magnetic sector field of opposite curvature direction. With this geometry, all ions of a mass spectrum could be 'double-focused' in a plane in the magnetic sector field, and thus could be detected simultaneously on a 25 cm long photo plate. This instrument already provided a mass resolution of 6500.

Since electrostatic sector fields are focusing ions with different energies to a single point, it is evident that double-focusing instruments are perfectly suited for a combination with ion sources generating ions with a broad energy distribution, such as glow discharge or inductively plasma sources. With the development of mono-energetic electron impact ion sources, single magnetic sector instruments became powerful alternatives to the relatively bulky double-focusing devices. For instance in 1940, Nier[23] designed a 60° single magnetic sector field instrument, which became commercially available as the famous CH4 gas analyzer from Atlas MAT GmbH. Using his apparatus, Nier enriched μg amounts of ^{235}U from uranium of natural isotope composition, and this type of instrumentation was widely used in the Manhattan project (1940 to 1945).

In 1942, Nier constructed a 180° sector field instrument, which became commercially available for organic analysis using an electron impact ion source. Most modern sector field devices are based on a theory first discussed by Alfred O.C. Nier and Edgar Johnson in the early 1950's, known today as Nier–Johnson geometry.[24] They reasoned that it would be easier to obtain second order double-focusing at a single point, a slit, rather than across a plane, as in the Mattauch–Herzog geometry. In the Nier–Johnson geometry, the 90° electric sector is arranged symmetrically and the 60° magnetic sector asymmetrically in the same curvature direction (see section 4.4). This geometry accepts a large divergence angle of the ion beam and guarantees second-order directional focusing. The Bainbridge–Jordan or Hinterberger–Konig geometry consists also of an electric sector followed by a magnetic sector with the same direction of curvature.

Modern commercially available GD- or ICP-SFMS systems are based on reverse Nier–Johnson (GD-SFMS, ICP-SFMS), forward Nier–Johnson (ICP-SFMS, GD-SFMS, MC-ICP-SFMS) or on Mattauch–Herzog (MC-ICP-SFMS) geometry. In the following text, the development of instruments based on glow discharge or inductively coupled plasmas will be discussed separately.

2.1 Glow discharge mass spectrometry (GD-MS)

A glow discharge (see section 5.1.1) source, producing both atoms and ions, is well suited for mass spectrometry; it was used for the first time already in the early days of mass spectrometry by the pioneers Aston, Thomson and Dempster.[25–27] Later on, due to the development of the electron impact ionisation, vacuum arc and spark discharges for ionisation in mass spectrometry, the analytical interest in glow discharges increased. For at least 25 years, beginning early in the 1960s, spark source mass spectrometry (SSMS) based on the Mattauch–Herzog geometry dominated solid source mass spectrometry.

SSMS provided extremely low detection limits at sub ng g^{-1} levels and its true multi-element capability.[28] The disadvantages were poor precision (>10%), resulting from a discontinuous operation of the radio frequency (rf)-sparks. The accuracy was insufficient for many applications and the use of photo-plates for detection was very laborious and time-consuming.

Due to these important limitations, researchers started to look for continuous discharges, such as arcs and glow discharges. The revival of the latter as ion source for mass spectrometry was initiated by Coburn, who used a planar diode sputtering arrangement (Glow Discharge), coupled to a quadrupole mass filter.[29] Later, he and his co-workers extended their work to rf-discharges for the direct analysis of both conducting and non-conducting solids and were even able to analyse Teflon in their first work.[30]

W.W. Harrison, who started with SSMS, but was looking for an alternative plasma discharge, contributed significantly to the development of GDMS. A hollow cathode direct current (DC) GD ion source was coupled to a SSMS instrument by Harrison and Magee[31] in 1974 and a couple of months later, a publication followed by Colby and Evans.[32] Only one year later, Harrison and co-worker started to explore rf-glow discharges, again using the SSMS instrument.[33] Over the years, rf-sources were strongly promoted by Ken Marcus,[34] but this is discussed in more detail in a review article.[35]

The first commercial glow discharge instrument, the *VG 9000* (VG Elemental, Winsford, UK), was based on a sector field organic mass spectrometer; it was introduced in 1985 and with the first analytical results appearing in 1986.[36] In its simplest form, GD consists of two electrodes with one electrode being the sample. The *VG 9000* was often operated with the sample being a pin and the cell including the sample was cryogenically cooled. Other source designs were developed for flat samples, thus allowing for depth profiling analysis and also became commercially available.[37]

A number of GDMS instruments were introduced in the following 20 years including a second sector field device from Kratos Instruments, several quadrupole-based instruments from VG Micro Trace (Winsford, UK), Extrel (Pittsburgh, USA) and Turner Scientific (Appleton, UK). Thermo Instruments (now Thermo Fisher Scientific, Bremen, Germany) offered an add-on GD source for their ICP-SFMS instrument (*Element*). The *Element* was also used in combination with a home-built rf-GD source by Becker and co-workers for the analysis of non-conducting samples[38] and it should be mentioned that a similar source was also coupled to an SSMS instrument.[39] By use of the *Element*, they achieved detection limits in low mass resolution mode of 10 ng g^{-1} for B in GaAs, but they were limited by memory effects arising from material deposited in the first lens of the mass spectrometer.[40]

Except for the *VG 9000*, further instrumental approaches disappeared quickly, leaving room for further instrumental developments. The need for further improvements finally led to the launch of a new research project and the development of the *Element GD* in 2005.

These improvements were mainly attributed to one limitation of the first generation of instruments: Due to the low discharge power (a few Watts only), the time needed to achieve stable signals under equilibrium conditions and the slow analyser, an analysis took as long as an hour or even more for some difficult-to-analyze ultra-pure materials. Thus low sample throughput was seen as one of the most limiting factors in GD-MS. In optical emission glow discharge spectroscopy, sources are operated with a power of up to 100 W and thus, a typical analysis time is not longer than 5 min. Therefore, improvement of the GD sources for MS instruments was required. Some of the most successful sources are based on a special geometry: the Grimm-type design. Sources based on this design principle have been convincing due to their stability, robustness and simple construction. This was the main reason for the development of new ion sources for MS, using design criteria well accepted in OES. The main advantage of the Grimm-type[41] source is that the flat sample itself served as the vacuum sealing part, thus enabling fast sample changing and source cleaning. Due to effective cooling, higher powers could be used and due to a restricted discharge area, this source turned out to be superior for bulk analysis in terms of stability in comparison to pin-type sources. Depending on operational conditions, flat-bottomed sputter craters could be achieved, so that depth analysis of multi-layered (high-tech) materials became a very important application for these sources. A Grimm-type source was first coupled to a quadrupole mass analyser.[42] The analytical performance of the system was originally characterized *via* the bulk analysis of steel standard reference materials using operational parameters selected based upon extensive optimisation measurements. The analytical results showed a satisfactory agreement with the corresponding certified values for 30 elements. The detection limit for multi-element analysis was about 0.1 μmol mol^{-1} and was 5 times lower for single element determination. The relative standard deviation (RSD) was in the range from 2% to 15%. With optimized working conditions (discharge power, pressure) the source was also deployed for depth resolved analysis.[43] Later, the same Grimm-type source was coupled to an ICP-SFMS instrument based on the prototype of the *Element*.[44,45] Overall, detection limits at ng g^{-1} levels and below were achieved.

Over the years, many attempts were made to improve the analytical figures of merit, as well as the sample handling of various GD sources. Significant improvements in sensitivity were achieved in GD-OES by applying a directed gas flow. In the latter case, the gas flow was directed onto the surface of the sample by using gas leading tubes or nozzles, so that a gas jet-assisted sputtering was achieved. In such a device, several processes contribute independently to the signal enhancement. First, the fast gas flow entrains sputtered atoms, greatly reducing lateral and back diffusion and thus, the transport of material to the region where the analytical signal is measured is improved. Additionally, the pressure is increased in front of the sample, so that the discharge power is concentrated onto a much smaller area. The concept of using a high and directed gas flow in GD ion sources was first investigated by Mason and co-workers for pin-type[46,47] and flat samples.[48,49] They calculated a minimum residence time of the gas flowing through their source of about 2.5 ms. This short residence time was the reason why they named it 'fast flow' (ff) source. Hoffmann[50] used the same concept, but with a modified Grimm-type source geometry operated in a DC- as well as in an rf-mode and coupled this source to a quadrupole mass spectrometer. In both experiments - by use of the 'fast flow' of the discharge gas (up to some hundred mL min^{-1}) - a significant improvement in sensitivity was observed. This was attributed to an overall improvement of the transport efficiency of ions into the mass spectrometer. Additionally, a suppression of polyatomic ion species by orders of magnitude was observed in comparison to mass spectra obtained by conventional MS sources with much lower gas flow. Bogaerts *et al.* showed by theoretical modelling of the Grimm-type source design[51] that the directed high gas flow rate improves transport efficiency of ions by gas convection, thus reducing diffusion losses to the wall.

In 2000, a consortium of researchers coordinated by Thermo Optek received European Community funding to develop a new glow discharge source based on the ff-concept for a new sector field instrument (*Axiom*). With the new source, the gas flow was demonstrated to result in an increase of the sensitivity combined with a suppression of polyatomic species.[52] In the corresponding paper, it was demonstrated that this concept is best suited for bulk analysis of conducting materials. It was shown that the matrix ion intensity exceeded that of argon by about a factor of 10, whereas under low power conditions with flow rates of far less than 1 mL min^{-1}, it amounted to 10% only. As a consequence, spectral interferences originating from the discharge gas were substantially suppressed at higher gas flow rates. Additionally, the sensitivity for most elements was improved by at least one order of magnitude in comparison to a 'static' source. Moreover, at such high gas flow rates, the pre-burn time required to get stable ion intensities could be reduced from 10 min to less than one minute, which could be attributed to the higher sputter rates, consequently leading to a fast equilibrium. Although developed for bulk analysis, a slightly modified gas flow in the source could be used to improve the sputter crater shape, but at a slightly reduced sensitivity. A flat crater bottom is a pre-requisite for successful depth-profiling. The sensitivity and the depth resolution achieved are sufficient for the analysis of high-tech multi-layered materials with layer thicknesses in the μm range. A fast flow GD source with a flexible modular design, enabling both dc- and rf-operation by switching the power supply only, was developed recently.[53]

A fast flow GD source with a concentric flow tube (for more details see section 5.2.1.2), is now used in the *Element GD* instrument (see section 5.2.1.2). In 2008, MSI introduced an updated version of the Kratos Concept GD, the *Autoconcept GD-90*, which offers an rf-mode. In 2010, Nu Instruments launched a new glow discharge mass spectrometer. The *Nu Astrum* is based on the *AttoM* ICP-MS and is equipped with a low pressure static discharge for maximum stability with high sensitivity tantalum cell for ease of cleaning.

For completeness, it should be mentioned that an alternative approach for GD-SFMS uses the Mattauch–Herzog geometry, allowing a simultaneous detection of all ions, but instead of photo plates, Hieftje and co-workers used an electronic array detector for simultaneous detection of all ions at the same time.[54]

2.2 Inductively coupled plasma mass spectrometry (ICP-MS)

One of the most successful analytical plasma sources in emission as well as in mass spectrometry is the inductively coupled plasma (see section 5.1.1.1). The analytical inductively coupled plasma (ICP) was described in 1964 by Greenfield[55] and later introduced for analytical applications in atomic emission spectroscopy (AES). The first commercial instrument was constructed in 1974. A year later, Alan Gray started to couple a quite different atmospheric plasma ion source to a quadrupole mass spectrometer, a combination *via* which first mass spectra were obtained for sample solutions.[56] However, the breakthrough of atmospheric pressure ion sources was achieved in the Fassel group at Iowa State University. Fassel was already a pioneer of the use of ICP in emission spectroscopy, to which he contributed a novel torch design.[57] In the group of Fassel, Houk started in 1978 to couple an ICP to a quadrupole-based mass analyzer in the context of his PhD work.[58] First results were published already in 1980, the official birth year of ICP-MS.[59] In the following years, papers from Gray and Date[60] and from Houk and co-worker[61] demonstrated the analytical performance of the prototype devices. In particular Houk and co-workers continued their pioneering work by providing the analytical community with many fundamental studies and novel applications (for more details, the reader is referred to the books previously cited[6,7,9,10]).

2.2.1 Single collector sector field instruments (ICP-SFMS). Commercialisation of ICP-MS was driven by two companies: VG Instruments in the UK and Sciex in Canada. However, only VG pursued the development of ICP sector field instruments based on their existing sector field organic mass spectrometers. Thus, existing technology was adapted for the development of plasma-based magnetic sector field instruments and in 1983, the first instrument based on a glow discharge ion source, the *VG 9000* was introduced in 1985, as discussed previously. The basic instrumental design originated from the *VG series 70*, a high resolution mass spectrometer with Nier–Johnson geometry used for analysis of organic compounds. The first sector field instrument with an ICP source followed in 1988 (*Plasmatrace*), also using the *VG 70*. In 1992, the first MC-ICP-SFMS was introduced (*Plasma 54*). JEOL introduced the *JMS-Plasmax* ICP-SFMS in 1993 (followed by *JMS-Plasmax 2* in 1995) which, like VG's *Plasmatrace*, was based on a previously existing organic mass spectrometer. The JEOL instruments were not successful outside of Japan (only one was sold to Egypt) and the series was discontinued.

The very high purchase price and the complexity of operation were the main issues why the first double-focusing instruments were not widely adopted. This fact served as an incentive for Finnigan MAT to apply for third body funding to develop a novel 'plasma monitor' based on a sector field instrument.

The main design criterion for this instrument was a smaller magnetic sector with a radius of 16 cm in a reverse Nier–Johnson geometry, resulting in reduced production cost and thus, lower price without compromising analytical figures of merit. The instrument could achieve a mass resolution of 3000 in the medium and 7500 in the high mass resolution mode, which enables most of the commonly encountered interferences to be resolved. The first hardware of this new instrument was already assembled at the end of 1991, but it took some further time to commercialize the instrument. The resulting instrument, the *Element*, was presented in 1993 and was introduced to the market in 1994.[62–65] An improved version of this instrument, the *Element 2*, was launched in 1998.

Other instruments were launched to the market as well, but not all are still commercially available. Thermo Optek, after it had acquired the assets of the former VG Elemental subsequent to Thermo's acquisition of Fisons Instruments, introduced a new ICP-SFMS, the *Axiom* in 1998. The *Axiom* was discontinued in 2002, leaving the *Element 2* and the closely related model, the *Element XR* (introduced in 2004) as the only commercially available ICP-SFMS for some time. In 2004, Nu Instruments introduced a new high resolution double-focusing sector field instrument, the *Nu Plasma*, which like the *Plasmatrace* and *Axiom*, had a continuously variable slit system which could cover resolution settings between 300 and more than 10 000. More instrumental details of currently commercially available instruments will be given in section 5.

2.2.2 Multi-collector ICP-SFMS. A limitation to the precision of isotope ratio measurements by scanning single collector instruments is the time-staggered detection, by which one isotope is measured after the other, resulting in reasonable precisions only. To overcome this limitation, multiple collector instruments were designed to allow static simultaneous detection of all isotopes of interest at the same time, by which instabilities of the plasma (flicker noise) or the sample introduction or drift of the signal intensity are no longer substantially affecting the isotope ratio, thus resulting in a significantly improved isotope ratio precision.

The first MC-ICP-SFMS instrument, the *Plasma 54*, was a hybrid of the VG *Plasmatrace* ICP-SFMS combined with the multi-collector system of the *Sector 54* TIMS (thermal ionization mass spectrometer). This instrument with an S-type-geometry consists of two electric sectors – before and after the magnetic sector – with a radius of 54 cm (*Plasma '54'*). It was equipped with an array of adjustable Faraday collectors for precise isotope ratio measurements and a Daly detector for ion counting. In this design, the ICP and interface were floating at high potential, while the rest of the instrument was operated at ground potential. The first isotope ratio measurements with this instrument were published by Walder *et al.*[66] in 1992 and already one year later, an application was shown for direct analysis of solid samples by use of laser ablation as sample introduction.[67]

While only a few units were sold, the potential of such an instrument was realized to be high. Micromass (the inorganic mass spectrometry assets of which were later acquired by GV instruments), a management buyout of some technologies from Fisons Instruments, introduced the *Isoplasmatrace* (later renamed the *IsoProbe*), which was based to a certain extent on technology of the *Plasmatrace 2* (ICP and front end design) and the magnet and collector array from the *Sector 54* TIMS. This instrument is a single magnetic sector field device only. Energy focusing is achieved by use of a hexapole collision and reaction cell in front of the magnetic sector.

Phil Freedman took the experience gained with the *Plasma 54* and started to design a completely new MC-ICP-SFMS with the newly founded company Nu Instruments in 1995. The *Nu*

Plasma was introduced in 1997 and the instrument was discussed in a publication by Belshaw *et al.* in detail.[68] The instrument is based on a Nier–Johnson double-focusing geometry and uses a fixed detector array in combination with zoom optics. Later, deficiencies in the instrument were corrected with the addition of a high resolution slit system (*Nu Plasma HR*). In 2010, it was replaced by *Nu Plasma II*. A larger geometry instrument, the *Nu Plasma 1700*, was introduced in 2002. The large geometry and large dispersion provides mass resolution of up to 5000 by full transmission while maintaining flat top peaks.

Thermo Optek added a multi-collector array to the *Axiom* to make the *Axiom MC* in 1998, which was later distributed by Thermo Elemental. This instrument is no longer commercially available. Thermo Quest (now subsumed into Thermo Fisher Scientific) introduced the *Neptune* in 1999, which uses the ICP interface of the *Element 2* and the multi-collector technology of a TIMS instrument (*Triton*, Thermo Fisher Scientific) and combines high mass resolution, variable multi-collection, zoom optics and multiple ion counting (MIC).

The main feature of multi-collector devices is the capability for a simultaneous detection of isotopes by use of discrete detectors. Over the years, the number of Faraday cups increased significantly and more and more, secondary electron multipliers were fitted into the instruments. This can be seen as answer to the fact that the use of Faraday cups limited the concentration range of the isotope of interest to higher ng g^{-1} levels. This drawback became even more evident when laser ablation was applied for direct sample introduction. Small analytical quantities resulted in low signals and poor isotope ratio precisions. In addition, the introduction of high resolution systems (slit systems) again reduces the sensitivity. Nonetheless, the number of analyzed isotopes is still limited reducing the multi-isotope capabilities especially on short transient signals (*e.g.*, with LA-ICP-MS). In principle, it is possible nowadays to design small cups by micromachining, so that all isotopes can be measured continuously as they are separated by a magnet and imaged simultaneously at the same focal plane. This idea is not new and was realized by using a double focusing sector field device with Mattauch–Herzog geometry. This design is promising because all ions are focused in a single plane.[69] In a collaboration of the groups of M. Bonner Denton, Gary Hieftje and Dave Koppenaal, an array of micromachined Faraday cups was developed which were used to cover the whole focal plane area of a Mattauch–Herzog type mass spectrometer. This is the reason why this detector was given the name 'focal plane camera'.[70,71] Special low capacitance integrating amplifiers are applied for signal amplification and the time resolution realized so far is already in the range of 1 ms $image^{-1}$ (see ref. 70). Hieftjes group had pioneered the technology for many years and they demonstrated that such a concept works for various types of plasma sources, including GD[72] and ICP ion sources.[73]

A commercial Mattauch–Herzog instrument with an ICP ion source and a focal plane camera was discussed in 2010 at the "Winter Conference on Plasma Spectrochemistry" in Fort Myers[74] and was introduced as *Spectro MS* to the market a few weeks later at the Pittcon conference by the company Spectro Analytical Instruments (Kleve, Germany).[75]

More details of today's commercially available instruments mentioned in this section will be given in section 5.

3 Fundamentals

3.1 Spectroscopic interferences

30 years after the famous publication of Houk, ICP-MS has matured to become one of the most important methods in atomic spectroscopy. There are many reasons for this success, but the most important are the extremely low detection limits achievable and the true multi-element capabilities. Although even nowadays the instrumental market is dominated by quadrupole mass spectrometers with approximately unit mass resolution, the current generation of ICP-SFMS instruments has a broad user base and has found widespread adoption by metrology labs, nuclear research and production facilities, chemical oceanography and geochemistry research groups and for diverse industrial applications, especially in the semiconductor industry. Over the years, the applications in the field of ICP-MS changed from rather pure to extremely complex samples and soon the old Achilles' heel of ICP-MS, which was described already in the first paper of Houk, was discovered again: the limitation by spectroscopic interferences.[76] As a consequence, high mass resolution was discovered as the most general principle to overcome this limitation.

Spectroscopic interferences may be subdivided into several groups, as they can be attributed to the presence of isobaric atomic ions, multiply charged ions and polyatomic ions of various origins. Isobaric overlap exists when the signals of nuclides of different elements coincide at the same nominal mass. Since the mass difference between isobars is in general very small, resolutions between 10^4 and 10^8 are required. The maximum mass resolution setting of commercial ICP-SFMS instruments (about 10^4) is by far not sufficient to overcome interferences of this kind. Therefore, an alternative approach to cope with this problem is used. For each element – with the only exception of indium – at least one isotope is free from isobaric overlap and can be monitored instead, but in many cases this will not be the most abundant one. This strategy is often successful. If more complex samples are analysed, the number of analyte signals disturbed by other kinds of interferences is drastically increased in the mass range below 100. Since isobaric interferences are usually easily predictable, they can also be corrected mathematically by using the natural isotopic abundances.

Multiply charged ions will be found in the mass spectrum at a position m/z (m is the nominal mass and z is the ion charge), *i.e.*, for instance doubly charged ions are found at half of their nominal mass. Multiply charged ions have usually a smaller formation rate in an ICP and occur mainly in the medium mass range. Doubly charged ions of the main matrix constituents are frequent contributors.

Among the spectroscopic interferences, polyatomic ions cause the most severe problems and thus their origin shall briefly be discussed. Polyatomic interferences are less predictable and depend on the sample composition (analytes and matrix) and the operational parameters of the ICP-MS system. Therefore, it is difficult and sometimes impossible to correct them mathematically. They require mass resolutions of 10^3 to 10^4 up to mass 70 and sometimes more than 10^4 at higher masses. Polyatomic interferences may be introduced by the sample itself, such as oxide ions which, owing to their high bond strength, have a real chance of 'surviving' the passage

through the hot zones of the plasma. They may also arise from the discharge gas, contaminants, entrained air, the reagents and solvents used and the matrix of the sample. They might become extremely complex in organic matrices.[77] The formation of cluster ions from the dominant species in the plasma (Ar, H, O, C, N) is a major source of polyatomic interferences and they occur preferentially in cooler plasma boundaries (possibly at the walls of the skimmer)[78] or in the sampling and expansion areas of the interface. Nonose and Kubota investigated the optical characteristics of micro plasmas behind the sampler and skimmer cone and observed an influence of the acceleration voltage on the formation of polyatomic interferences, as well.[79]

Many approaches to cope with the problem of spectral interferences have been discussed in literature and will be covered later on in this paper as well. Most of them are limited to some specific interferences or are applicable for some selected matrices or elements only. The most straightforward method to overcome limitations from spectroscopic interferences is the application of high mass resolution as the interfering ion can be separated and monitored directly in the mass spectrum. The mass resolution $m/\Delta m$ is commonly defined according to the 10% valley definition for sector field instruments, where Δm is the mass difference between two adjacent peaks of equal height that are separated by a valley which is 10% of the peak height at its lowest point. The high mass resolution capability of ICP-SFMS allows the identification of interferences and ions of interest on the basis of their exact mass easily and from these experiences we can already define major groups of possible spectroscopic interferences and some of their features:

Ar-containing ions

• Ar is introduced for plasma generation at flow rates between 15 and 20 L min^{-1}.

• Under standard plasma conditions, Ar^+ and Ar_2^+ are always observed as very intense signals, thus affecting detection of K^+ and Ca^+ and Se^+.

• Ar^+ can form polyatomic species with elements from the solvent, ambient air and/or the matrix of the sample

Analyte M attached to oxide and hydroxide ions

• m/z + 16 (MO^+) and m/z + 17 (MOH^+) are typical interferences

• The ratio of MO^+/M^+ depends on the M–O bond strength

• Usually it is observed that $MO^+/M^+ > MOH^+/M^+$

• By optimization of the instrumental settings, the formation of (hydr)oxide ions usually can be reduced to values of $MO(H)^+/M^+ < 5\%$

• The interference is a major problem if m/z (M_1O^+) = m/z (M_2) and $c(M_1) > c(M_2)$

• (Hydr)oxide interferences are formed in the ICP or 'survive' the ICP in regions with low temperatures (*e.g.*, in the neighbourhood of vaporizing droplets, particles)

Doubly charged ions

• The degree to which M^{++} ions are formed depends on the difference between the 2nd and the 1st ionization potential of the element

• Ions of this type always have a strong effect once they are present as major components of the sample, solvents or the discharge gas, for instance

• *E.g.*, $^{138}Ba^{++}$ can hamper the detection of gallium.

• The formation of M^{++} strongly depends on the working conditions and can be reduced by application of a shield between the plasma and the induction coil to reduce capacitive coupling of the high frequency.

Solvent and matrix based polyatomic ions

The most severe spectral interferences observed in many applications most often belong to this group

• They are formed by constituents of the solvents used and can take the form of: MCl^+, MC^+, MSO^+, MNO^+

• Or by components of the matrix such as: MNa^+, MCa^+, MK^+

The formation of interferences is governed by thermodynamics (exothermic and endothermic processes) and is possible if the energy which is needed for the process is provided by the plasma or the excess reaction heat. The product molecule usually has a binding energy which is high enough to survive the short passage through the plasma and the interface as exposure time of particles in the plasma is only about 5 ms.[80] This is also the reason why polyatomic species with low binding energy such as ArH_2O^+ and $Ar\,H_3O^+$ are not detected. If molecules of this kind are measured in the mass spectrum, this would give us a hint that they are formed in an environment with much lower temperatures. This idea was used by Sam Houk to study the origin of most spectroscopic interferences.[81]

3.2 How to cope with spectroscopic interferences

As a first conclusion, we can say that a proper optimization of the instrument is the very first step and most efficient way to overcome interferences at the first instance and is even a prerequisite in sector field mass spectrometry as it even may help to avoid operation of the instrument in a high resolution mode, with its inherent loss in sensitivity. Nonetheless, there are several strategies to cope with residual interferences besides the use of high mass resolution. The alternatives will be described shortly in the following sections. High mass resolution will be discussed in more detail in sections 3.3. and 3.4.

3.2.1 Mathematical correction procedures. Mathematical correction is usually applied in case of simple corrections (isobaric interferences) or if all other measures fail. In case of isobaric interferences, the interfering element is measured at another isotope mass along with the analyte of interest and the contribution of the interference is calculated *via* the isotopic abundances.

The situation is more complicated for polyatomic interferences as they are not easily predictable and depend on the operational parameters as well as on the matrix. Therefore, the formation probability has to be estimated using external matrix-matched solutions or the same interference has to be observed on a different mass and used for further correction.

This is demonstrated *via* the following example: $^{75}As^+$ suffers from a spectral interference in Cl-containing solutions as a result of the occurrence of the $^{40}Ar^{35}Cl^+$ ion. As a consequence, the following mathematical strategies can be used:

The $^{40}Ar^{35}Cl^+$ interference is measured along with the $^{35}Cl^+$ (or $^{37}Cl^+$) signal in pure matrix solutions containing only the matrix and Cl of increasing concentration, but with no As. The ratio $^{40}ArCl^+/^{35}Cl^+$ is calculated from these solutions and an average ratio is further used as correction factor. Now, the signal

on mass 75 is measured in the solution along with the signal of $^{35}Cl^+$ on mass 35 (or $^{37}Cl^+$ on mass 37). The $^{35}Cl^+$ (or $^{37}Cl^+$) signal is now multiplied with the previously calculated factor resulting in the probable interference of $^{40}Ar^{35}Cl^+$ on mass 75. The remaining signal is most probably the requested As signal.

Another possibility would be that the $^{40}Ar^{37}Cl^+$ signal on mass 77 is measured along with the signal on mass 75. *Via* the isotopic abundances of Cl, the $^{40}Ar^{35}Cl^+$ signal can be calculated from the $^{40}Ar^{37}Cl^+$ signal. Again, the remaining signal is most probably the requested As signal. Nonetheless, we can observe an additional problem: We find also $^{77}Se^+$ on mass 77 where we expect our $^{40}Ar^{37}Cl^+$ interference. Therefore, we have to subtract the signal of $^{77}Se^+$ prior to calculate the $^{40}Ar^{35}Cl^+$ from the $^{40}Ar^{37}Cl^+$ signal. We can correct $^{77}Se^+$ *via* the isotopic abundances using, *e.g.*, the $^{82}Se^+$ signal. Nonetheless, we have to consider that we find an isobaric interference of $^{82}Kr^+$ on mass 82. Not to consider any $^{40}Ar_2{}^1H_2{}^+$ interference. It is obvious that this strategy leads only to satisfying results when a relatively high analyte concentration and low matrix concentration are occurring.

As good strategy, it is always wise to monitor more than one isotope (if possible), even if the other isotopes are less abundant.

3.2.2 Sample introduction systems. Among various strategies discussed over many years, the appropriate selection of a sample introduction system best suited for the analytical problem can already help to overcome many solvent- and matrix-based spectral interferences. Cooled spray chambers are applied to reduce the amount of water vapour transferred to the plasma. Systems use heating/cooling devices in order to condense and drain the solvent. Advanced systems use desolvation systems to significantly reduce interferences.[62] Solvent molecules can pass through membranes and are removed by a counter stream of Ar, whereas the dried aerosol is transported to the plasma. *E.g.*, oxide formation rates can be reduced by some orders of magnitude compared to conventional introduction systems. Depending on the temperature programmes chosen for electrothermal vaporization, solvent-based interferences can be reduced in advance to the analysis of the trace elements. We refer to a recent review for more details.[82]

Dissolution of solid samples and thus interferences caused by mineral acids can be avoided if laser ablation is chosen as a sample introduction device, even though other matrix-based interferences can occur. Also here, more details can be found in literature.[83]

3.2.3 Sample/matrix separation. One straight chemical method to avoid formation of interferences is the direct separation of the matrix from the analyte of interest. Even spectral interferences from samples with a high level of dissolved salts can be avoided if, *e.g.*, hydride or cold vapour generation is applied for trace/matrix separations.[84] The analyte of interest can be separated from the interfering matrix by chromatography as well. This is accomplished either by using a batch process or by direct coupling of chromatography to ICP-MS. A prominent example is the separation of Sr from the matrix as Ca- and P-containing polyatomic species along with the isobaric interference of Rb is causing significant difficulties in accurate Sr isotope ratio determination. Batch processes, ion chromatography or on-line separation using micro columns are applied.[85–87]

3.2.4 Cool/cold plasma technique. A number of interfering ions are formed directly inside the inductively coupled plasma or at walls in contact with the plasma. Thus, changing the working conditions of the plasma is a powerful tool for the reduction of especially argon-based interferences. This approach was realised in the 'cool/cold plasma' technology. This was accomplished by increasing the nebulizer gas flow rate or addition of an additional gas to the central channel of the torch, along with the reduction of the rf-generator power. In this operation mode, the risk of secondary discharges was high. The breakthrough was achieved once effective plasma shielding was developed by appropriate induction coil grounding or application of a plasma shield.[88]

The cold plasma technique helps to reduce argon-based spectral interferences such as Ar^+, ArC^+, ArO^+, $ArCl^+$, $Ar_2{}^+$. This can be used for an improvement of LODs for elements such as Ca, K, Cr, and Fe, which are of importance, but difficult to analyze at low levels, *e.g.*, in the electronic industry. These advantages have to be paid for under the form of many additional spectral interferences coming from water clusters (combinations with H_2O and H_3O) and increased oxide formation. Additionally, a loss in sensitivity for all elements with first ionization potential above 8 eV have been observed and even worse, a loss of robust plasma conditions causing elevated matrix effects hampers its application. As a consequence, mainly pure samples with low salt content can be successfully analyzed in this mode.

3.2.5 Collision and reaction cell technology. Among all approaches for overcoming spectral overlap, those based on instrumental improvements have been most successful and in particular, the application of collision and reaction cells in front of a low resolution quadrupole mass analyser have changed the whole spectrum of applications in ICP-QMS. Although at the beginning of this technology, the first experiments were very disappointing. For instance, Douglas investigated collision-induced dissociation for ICP-MS and found that the total loss cross sections for analyte ions and interfering molecules are of the same order of magnitude.[89] On the other hand, he showed in the same experiment that ion molecule chemistry occurring in a cell of a triple quadrupole arrangement is a more powerful approach to reduce spectral interferences generated by molecular ions. Similar experiments were performed in parallel by Rowan and Houk, using a MS/MS arrangement which consists of two quadrupoles.[90] Although the gas phase reaction and reduction of Ar-associated molecular ions had been demonstrated, the loss of ions from the first band pass quadrupole filter by scattering of analyte ions as a result of their collision with background gas made a practical use questionable. The breakthrough came with multi-pole arrangements, in which collisions proceeding in the reaction cell are stabilizing the ion beam on axis of the multipole arrangement. This was used by Eiden *et al.*[91] and later by Turner *et al.*[92] In both investigations, the reaction chemistry of H_2 for reduction of Ar-related molecular ions was investigated in more detail, demonstrating that this approach is efficient for the interferences of interest (see also ref. 93).

In current cell technologies, a pressurized cell, equipped with an ion guide (which – depending on the instrument – is an rf-only band-pass quadrupole, a hexapole or an octopole) is used to overcome a number of prominent spectral interferences by gas phase reactions with a reaction gas (reaction cell) or by

application of retarding fields in combination with a collision gas (collision cell). In the latter case, molecular polyatomic species are expected to lose more kinetic energy by collisions with a buffer gas. With application of a retarding field, their loss is higher compared to that of the analyte ions (kinetic energy discrimination). Reaction gas technology is based on the formation of different molecular ions form the interfering polyatomic species (*e.g.*, $2ArAr^+ + H_2 \Rightarrow 2ArArH^+$), neutralisation of interferences (*e.g.*, $Ar^+ + NH_3 \Rightarrow Ar + NH_3^+$) or by making use of shifting the analyte of interest to a higher mass (*e.g.*, $^{32}S^+$ to $^{32}S^{16}O^+$ using O_2 as reaction gas). Usually reaction gas technology is advantageous to be coupled with an ion filter in order to exclude newly formed interferences. All reactions depend on gas phase thermodynamics and even though they can be predicted in theoretical approaches, optimization is usually based on empirical parameters. More details of gas phase reactions taking place in these collision/reaction cells are discussed in a comprehensive review article by Tanner *et al.*[88]

Nevertheless, also a single reaction or collision gas or application of the combination of a buffer gas and a retarding field is not able to overcome all possible interferences from polyatomic species and most often, the interfered element has to be analysed in a separate run to achieve the best sensitivities for as many elements as possible. Moreover, the matrix dependence of the reaction/collision cell technology is not fully elucidated. Nonetheless, the technology has especially its advantage over high resolution ICP-SFMS if the requested resolution is more than 10 000. As an example, Sr and Rb were separated using reaction cell technology by shifting $^{87}Sr^+$ to $^{87}Sr^{19}F^+$ by applying CH_3F as reaction gas.[94] In principle, collision cells are also suitable for ICP-SFMS, as it was commercialized in the *IsoProbe* MC-ICP-SFMS, where a collision cell is used for energy focusing in a single focusing sector field instrument (magnetic sector only).

3.3 Mass resolution

Whether or not an interfering ion signal will be separated from an analytical signal depends on the mass difference and the resolution of the instrument.

Mass resolution R is generally defined as

$$R = \frac{m}{\Delta m} \qquad (3.3.1)$$

where Δm is the mass difference necessary to achieve a valley of 10% between two neighbouring peaks of identical intensity at mass m and $m \pm \Delta m$ as shown in Fig. 2.

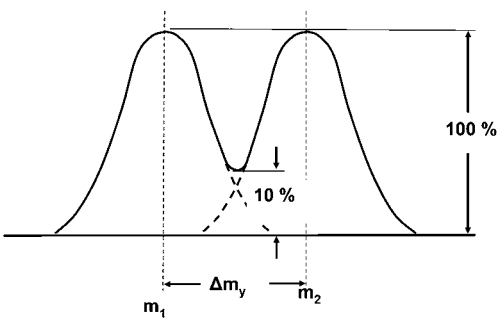

Fig. 2 10% valley definition of mass resolution.

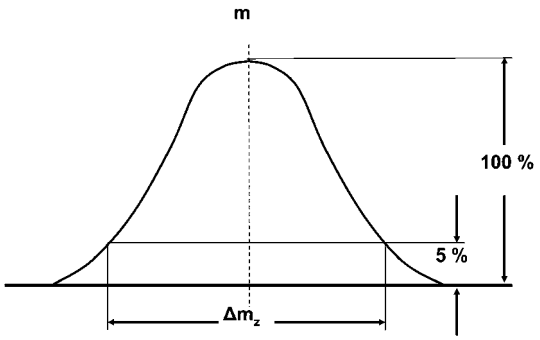

Fig. 3 5% definition of mass resolution.

However, since the intensities of two neighbouring peaks are rarely identical, an alternative definition is much more useful in practice. In this definition Δm is determined from the peak width at 5% of the peak height of a single interference-free peak (Fig. 3). For Gaussian peaks this will lead to the same value as in the 10% definition. Quadrupole-based mass spectrometers do not lead to Gaussian peaks and the mass resolution is usually determined by using the full-width at half maximum definition (FWHM, Fig. 4). For other instruments, such as time of flight mass analyzers, the full width at half maximum (FWHM) is usually used as well. The numerical resolution values based on the FWHM definition are about twice as high compared to the 10% valley definition. More details are given in section 6.1.2. Finally, MC-ICP-SFMS are operated frequently at edge resolution (see section 6.2.3).

In Table 2, selected examples are given for the most frequent spectral interferences caused by various solvents commonly used in ICP-MS. This table shows the most commonly investigated elements with their major abundant isotope(s) and the most frequent interferences. Low abundant interferences are excluded. As can be seen from this table, most polyatomic species can be separated from the nuclide of interest by application of high mass resolution ($m/\Delta m < 10\,000$). In most of the relevant examples of spectral interference, a resolution of about 4000 (most often called medium resolution) would be by far sufficient for baseline separation. Only in special cases, some polyatomic species are observed, which require a higher mass resolution ($4000 < m/\Delta m < 10\,000$). In the example given for ^{75}As in Table 2, such interference is caused by chlorine which in combination with Ar from the discharge gas can cause interference at the nominal mass 75.

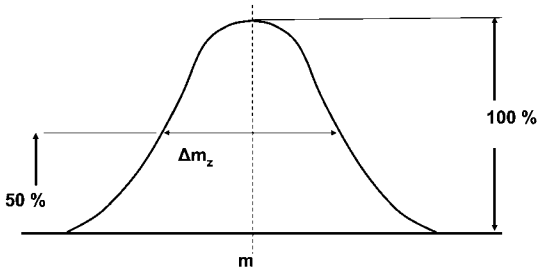

Fig. 4 Full width at half maximum (FWHM) definition of mass resolution.

Table 2 Selected typical polyatomic interferences in ICP-MS and required mass resolution to separate the nuclide of interest from the interfering polyatomic ion

Nuclide	Polyatomic ion	Resolution
$^{28}Si^+$	$^{14}N_2^+$	958
$^{31}P^+$	$^{14}N^{16}O^1H^+$	968
$^{31}P^+$	$^{15}N^{16}O^+$	1458
$^{52}Cr^+$	$^{35}Cl^{16}O^1H^+$	1671
$^{32}S^+$	$^{16}O_2^+$	1801
$^{64}Zn^+$	$^{32}S^{16}O_2^+$	1952
$^{54}Cr^+$	$^{40}Ar^{14}N^+$	2031
$^{54}Fe^+$	$^{40}Ar^{14}N^+$	2088
$^{56}Fe^+$	$^{40}Ar^{16}O^+$	2502
$^{48}Ti^+$	$^{32}S^{16}O^+$	2519
$^{51}V^+$	$^{35}Cl^{16}O^+$	2572
$^{44}Ca^+$	$^{28}Si^{16}O^+$	2688
$^{64}Zn^+$	$^{32}S_2^+$	4261
$^{75}As^+$	$^{40}Ar^{35}Cl^+$	7775

A resolution of about 8000 is sufficient to overcome this problem.

Of course, high mass resolution is not a panacea against all spectral interferences. As mentioned already, isobaric interferences are far beyond the scope of most commercially available devices besides others. For instance, MO^+ ions, where oxygen is a constituent of many mineral acids and water, can cause problems in the mass range below 100 u and above 140 u, and a resolution of less than 10 000 is sufficient for a complete separation. In the mass range between 100 and 140 u, a resolution of up to 1 000 000 would be necessary. The required resolution exceeds by far the resolution attainable with commercially available instrumentation. This is a crucial point for, *e.g.*, low level rare earth element (REE) analysis if formation of oxides is not prevented by other means. This example demonstrates that high mass resolution is a very powerful approach to overcome many, but not all of the spectral interferences occurring in routine applications.

3.4 Instruments with high mass resolution

High mass resolution of sector field instruments is a feature which depends on the geometry of the electric and magnetic sector, and the slit configuration (see section 5). However, high mass resolution is not a capability exclusive to sector field instruments, because other analyzers, including quadrupoles can be operated at higher mass resolution. Conventionally ICP-QMS instruments provide approximately unit mass resolution, but they can also be operated in higher regions of stability and reach for instance in the 2nd region of stability resolutions of up to 9000.[95] Another approach based on quadrupole instruments are tandem devices, with a subsequent series of quadrupoles. If both quadrupoles have reflecting grids, ions can be reflected in this trap many times and by multiple passes, resolutions of up to 20 000 were realized.[96] Another trapping concept is provided by ion traps and they have been investigated for their use in ICP-MS by Koppenaal.[97] They consist of a ring electrode in the centre, with two hyperbolic end caps above and below. They are operated with rf-voltages and are read-out by a high voltage pulse which injects the ions into a channeltron multiplier. Depending on the number of cycles the ions spent in the trap, the resolution achieved can be increased from $m/\Delta m$ 200 to 2000 (FWHM). A different type of mass analyzer applied in ICP-MS is the so called Time-of-Flight (ToF) analyzer, which has been investigated in Hieftje's group for a long time. They could show that if such instruments are operated with a reflectron to overcome differences in ion energy, they could be easily operated with a $m/\Delta m$ of up to 2200 (FWHM) in ICP-MS and GD-MS applications.[98] In ion cyclotron resonance Fourier transform (FT) analyzers, the ions are injected into a strong magnetic field and are gyrating on circles. The gyration frequency is depending on the mass of the ion and this frequency is picked up by a condenser-like detector. By transforming the frequency domain into a mass domain, an approach known as Fourier transformation, mass spectra are obtained. Resolutions in GD- and ICP-MS operation of $m/\Delta m$ of up to 100 000[99] and more than 1 000 000 (FWHM) have been reported.[100,101] A similar device in which ions are gyrating in a field, but this time an electrical, has been invented by Alexander Makarov[102] for organic applications and has become known under the trade mark: *Orbitrap*. Again, Fourier transformation results in mass spectra. Koppenaal started with a challenging experiment to use an *Orbitrap* in combination with a linear quadrupole ion trap with an ICP ion source. At the FACSS in 2009, he demonstrated that resolutions of $m/\Delta m$ up to 150 000 could be achieved.

As a summary, it can be said that instruments mentioned in this section are becoming more powerful and look therefore very promising for future ultra-high mass resolution applications, but so far they are not commercially available yet and thus will not be discussed here in more detail (a more detailed discussion is given elsewhere[7,9]).

3.5 Mass fractionation effects and isotopic variations

As mass spectrometers are isotope-specific, isotopic variations caused in nature or by fractionation in instruments have to be taken into account not only for isotope ratio analysis and will be discussed for this reason in more detail in this section.

The isotopic composition of elements is generally assumed to be invariant in nature and taken as constant. The natural isotopic variation is small, but existing for most isotopic systems. An overview of the isotopic composition and average masses are given in the IUPAC tables, which are updated on a regular basis.[103] For quantification by external calibration with total combined uncertainties of several percent (mainly influenced by repeatability, blank and calibration), the natural variation is, certainly in most cases, negligible. For quantification by isotope dilution, these variations have to be taken into account only for a limited number of elements (*e.g.*, Pb). Isotope ratio determinations on the other hand make use of the natural variations in order to use them in, *e.g.*, geochemical, environmental or technological applications.

Variations in nature but also variations in the isotopic composition induced by engineering and science are applied in many fields of science. Isotopic variations are based on mainly four different effects based on kinetic or thermodynamic reasons:

The first effect is radioactive decay or generally nuclear reactions. When one or more isotopes of an element are daughter nuclides of a radioactive decay, the isotope ratio(s) of the element depend on the original concentration of the mother nuclide in the

sample and the time. The natural radioactivity is, *e.g.*, used for dating *via* the half-life in archaeometry (*e.g.*, radiocarbon dating)[104–106] and geochronology (*e.g.*, U–Pb dating)[107–109] or for using the isotopic variation as natural fingerprint (*e.g.*, Sr, Pb).[110–113]

The second effect derives from simple mass-dependent thermodynamic processes (*e.g.*, evaporation), simply influenced by preferential diffusion of lighter isotopes. This can be observed for volatile elements or compounds (*e.g.*, H_2O, where, *e.g.*, the rain is getting isotopically lighter from sea towards inland by preferential precipitation of 'heavier water').[114,115] This effect can also be observed for other elements, such as Hg or Cd, in technical processes as well as during or after impacts of meteorites.[116,117]

The third effect is called isotope effect and refers to chemical reactions. The rate of a chemical reaction is defined by the activation energy, which is the difference between transition state and ground state of the reactant(s). Because molecules with different isotopes show different zero point energies, the activation energy is different and so is the reaction rate for kinetically controlled reactions. A good example is the reaction of breaking a C–H bond. In practice, the rate constant for breaking the C–H bond is 3 to 8 times higher than that for breaking a C–D bond.[118] Another possibility is if products differ by their ground energy and the reaction is ruled by thermodynamics, but not by kinetics as for boron. In aqueous solution, two boron species are present, $B(OH)_3$ and the $B(OH)_4^-$ anion. Here ^{11}B prefers the trigonal-planar structure of $B(OH)_3$, while ^{10}B prefers the tetrahedral structure of $B(OH)_4^-$.[119] In rocks preferably $B(OH)_4^-$ is being incorporated, so that $B(OH)_3$ remains in the aqueous phase, which leads to isotope fractionation in nature.[120] Fractionation of C, N or S in biological processes can also be guided by a combination of kinetic and thermodynamic effects, leading to significant natural variations.[121]

The fourth effect is 'artificial adulteration'. In technical and scientific applications, enriched isotopes are used or added to samples or systems to yield certain effects or to study certain processes. In the technical field, ^{10}B is used as neutron absorber in nuclear power plants working with pressurized water reactors. This is due to the very high neutron cross-section of ^{10}B, which amounts 3.84×10^3 barns and therefore exceeds 8×10^5 times that of ^{11}B.[122] In science, enriched isotopes are used for tracer experiments in biology and medicine,[123–126] or quantification in analytical chemistry applying isotope dilution mass spectrometry.[127,128]

Since effects 2 and 3 affect all isotopes of an element and lead to a shift in the isotopic composition, this process is denoted as isotope fractionation.

It is evident that mass fractionation induced by thermodynamic and kinetic effects occurs in all physical and chemical processes (to a different extent). Therefore, it is evident that mass fractionation also occurs in the mass spectrometer during measurement, *e.g.*, during diffusion of ions of different mass in the plasma, in the interface and during their way through the mass analyzer as a result of electrostatic repulsion (space charge effects) and collision with, *e.g.*, residual gas molecules (in the latter case it is obvious that significantly higher mass discrimination can be found in reaction or collision cell arrangements). From a physical point of view, a high acceleration voltage can reduce space charge effects, but nevertheless they can not be neglected even in sector field devices. The resulting difference in transmission efficiency for the isotopes of an element in ICP-MS is generally referred to as mass discrimination (additional details see section 6.3).

3.6 Background noise and abundance sensitivity

Abundance sensitivity normally refers to the contribution of an ion peak (at a particular mass), to an adjacent peak at lower or higher mass. Peak tailing is normally caused by small differences in the ion energy or different angles of motion compared to the ideal ion path of the ions. The latter differences are mainly caused by collisions of the ions with residual gas molecules in the analyzer region, thus a good analyser vacuum is essential, or by electrostatic repulsion of the ion beam itself (space charge) for intensive ion beams. Scattered ions are moreover generated at slits, apertures and the flight tube walls. Ions that suffered one of these interactions have lost kinetic energy and/or have changed their direction of motion. As a result, these ions appear at incorrect mass positions along the analyzer focal plane. For an intense isotope, the scattered ions can appear in the spectra even at neighbouring masses contributing to an elevated background. In order to reject these scattered ions, an electrostatic filter can be applied. It rejects scattered ions on the basis of both their lower kinetic energy and their irregular flight paths. In order to reduce the amount of such low energy ions, a retarding potential at a lens is applied and thus, the energy of the ions is reduced. Only ions above a particular energy threshold are passing this lens and are determined at the detector. These filters are positioned in front of a single multiplier, thus improving the abundance sensitivity for only that multiplier in a multi-collector arrangement. More details are given with the respective instruments in section 5.2.

Usually, in low mass resolution, the abundance sensitivity of sector field instruments is slightly worse in comparison to that of quadrupole-based instruments, but it is improved in high mass resolution mode.

As already mentioned, in comparison to quadrupole-based ICP-MS instruments, sector field devices excel by a number of features, among which the high mass resolution capability is the most important one. Additionally, these instruments show a much higher sensitivity and a much lower non-spectral background, so that the limits of detection are improved significantly. The improved sensitivity is often attributed to a higher transmission of sector field devices especially for high mass elements, for which losses are much higher in a quadrupole device. The lower noise background can be attributed to the bended geometry, as a result of which noise produced by fast neutrals or photons is very effectively suppressed. Moreover, magnetic sector field devices are operated under vacuum conditions, which are usually one to two orders of magnitude lower in pressure compared to quadrupole systems.

4 Theory

4.1 Magnetic sector

The magnetic sector is the core part of a sector field mass spectrometer. Its function can easily be explained with the help of the motion of a charged particle (electron, ion) in a magnetic field. Charged particles with charge q ($= ze$), velocity v and mass m injected into a magnet field B are forced by the Lorentz force

(perpendicular to direction of ion motion and magnetic field) onto a circular path with radius r_m.

$$qvB = m\frac{v^2}{r_m} \quad (4.1.1)$$

The centripetal force is then equal to the Lorentz force which gives

$$r_m = \frac{mv}{qB} \quad (4.1.2)$$

$$\frac{mv}{q} = Br_m \quad (4.1.3)$$

Therefore, the magnetic analyser is dispersive with respect to the mass and energy of the ions (or better the momentum), such that the magnetic analyzer is a 'momentum separator' and can be used for mass separation if all ions with different mass have the same energy. To achieve this condition to the best possible extent, the ions generated in the ion source are accelerated over a potential difference U_0 (the acceleration voltage), thereby minimizing the ratio of $\Delta E/E$ (ΔE = energy spread of the ions; E is energy of the ion). The kinetic energy of the accelerated ion is:

$$qU_0 = \frac{1}{2}mv^2 \quad (4.1.4)$$

and therefore:

$$r_m = \frac{1}{B}\sqrt{\frac{2mU_0}{q}} \quad (4.1.5)$$

$$\frac{m}{q} = \frac{B^2 r_m^2}{2U_0} \quad (4.1.6)$$

From eqn (4.1.6), it can already be seen, how a mass spectrum can be acquired:

• First, keeping B and r_m constant and changing the accelerating voltage U_0 results in a so-called electric scan (E-scan). Due to a loss in sensitivity and focusing properties (increase of aberrations), the mass range which can be scanned in this mode is usually limited to 30%–40% of the magnet mass. This operation mode can be used for fast scanning, because alteration and stabilisation of the acceleration voltage can be achieved very quickly and is independent of mass.

• Second, keeping r_m and U_0 constant but varying B results in a so called B-scan. In principle the mass range is unlimited and only dependent on the applied magnetic field, which is technically limited for iron core magnets to about 2 T. To retain sufficient field homogeneity for high mass resolution, a practical limit is more like 1.5 T. This still allows using ion energies of some keV. In comparison to other mass spectrometers, such as quadrupoles, this scan mode is slower, because the speed of magnetic field changes is limited by the self-induction of the magnet (eddy currents) and the power supplies needed. Therefore, a certain settling time is always necessary after changing the magnetic field. This settling time is depending on the magnitude of the change in magnetic field (required for 'jumping' from one mass to another) in a peak hopping mode. In practice, for signals corresponding to ions with masses within a relatively narrow mass range, the same magnetic mass is used. Scanning across a spectral peak is accomplished *via* E-scanning, followed by a jump of the electric field to the next mass followed by the next E-scan across the spectral peak of interest. When the scan range limit is reached, the magnetic field is adapted, resulting in a "jump" to a new magnetic mass. This mode is the preferred operation mode in scanning ICP-SFMS.

• The two previous ways to obtain a mass spectrum are mainly used for scanning single collector instruments but a third way, keeping U_0 and B constant, is the operation in static mode as used for multi-collector instruments, for instance Faraday cups located at different positions, corresponding to different r_m. This mode is always applied in multi-collector instruments for simultaneous measurements of the intensities of all ions monitored, thus providing high precision for isotope ratio analysis. Another way to use this concept is to place a detector array in the focal plane in instruments based on the Mattauch–Herzog geometry.

Eqn (4.1.6) shows already that the m/q scale is not linear, such that peaks of heavier ions are spaced more closely. For introduction of these equations, it is usually assumed that the magnetic field fills a whole plane area, but the electromagnets used in commercial devices usually have a specific sector geometry and thus, the magnetic field is restricted to a certain space or area.

A sketch of the geometry of a magnetic sector is shown in Fig. 5. It consists of an ion source, an entrance (alpha) slit, the magnetic sector with radius r_m, the collector (beta) slit and a collector/detector for instance a Faraday cup.

There are three basic features of a magnetic sector as an ion optic element: mass dispersion, angular focusing and energy dispersion, which will be briefly discussed in the following sections (more details are given in the following books[129–131]).

4.2 Dispersion

The term dispersion might be already known from optical spectroscopy, where it describes the power of refraction of a dispersive optical element, such as a prism, where the refraction is typically a function of the wavelength. In mass spectrometry, the magnetic sector is a mass dispersive element and therefore dispersion D can be defined as the physical separation distance Δr (*e.g.*, in mm) of two masses with a mass difference Δm along the focal plane in the region of the collector slit (the collector plane).

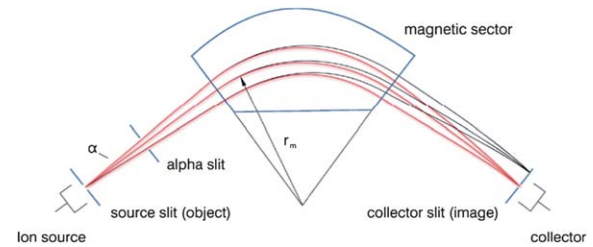

Fig. 5 Sketch of the geometry of a magnetic sector arrangement.

A magnetic sector has many physical properties which can be compared with "optical" devices and it best can be compared with a prism, because it has dispersive and magnification properties, depending on its geometry. For a magnetic sector with a 180° geometry, the dispersion at the focal plane at 180° is $2\Delta r$ (Fig. 6) when two ion trajectories of the same origin show a difference in the radii of Δr. Rewriting eqn (4.1.6) results in eqn (4.2.1) and differentiation results in the relation of Δr and Δm, the dispersion D (eqn (4.2.3)).

$$r_m = \sqrt{\frac{2U_0}{qB^2}}\sqrt{m} \tag{4.2.1}$$

$$\Delta r_m = \left.\frac{\partial r_m}{\partial m}\right|_{U_0,B} \Delta m \Rightarrow \Delta r_m = r_m \frac{\Delta m}{2m} \tag{4.2.2a–b}$$

$$\Rightarrow D = 2\Delta r_m = \frac{\Delta m}{m} r_m \tag{4.2.3}$$

It is clear that for a mass difference of Δm at mass m, the dispersion is $2\Delta r$, or in other words, for this geometry the dispersion is proportional to the magnet radius and indirectly proportional to the mass. This holds true for other geometries as well.

The dispersion in a general form can be written as

$$\Rightarrow D = \frac{\Delta m}{m} D_0$$

The dispersion coefficient D_0 is only depending on geometrical parameters of the magnet (angle of deflection, entrance angle, exit angle) and the magnitude is usually in the range of the radius of the magnetic sector.

The dispersion is an important parameter of a sector field instrument, because it is directly related to the resolution achievable with the device. During a scan, the ion beams of mass m and $m + \Delta m$ are moved across the collector slit. They are 100% resolved, when the ion beam of mass m already passed the slit and the ion beam of mass $m + \Delta m$ has not entered the slit yet. The slit widths of the entrance and collector (exit) slit are s' and s'', respectively. The distance between the centres of both ion beams is the dispersion D (Fig. 7) and the ion beam has the width b. Therefore, the dispersion can be expressed by eqn (4.2.4)

$$\begin{aligned} D &= s'' + b = D_0 \frac{\Delta m}{m} \\ \Rightarrow \frac{m}{\Delta m} &= \frac{D_0}{s'' + b} \end{aligned} \tag{4.2.4}$$

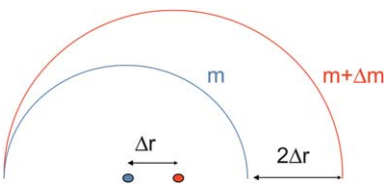

Fig. 6 Dispersion at the focal plane at 180°.

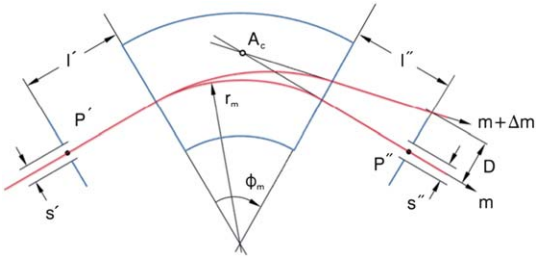

Fig. 7 Mass resolution in a magnetic sector field.

The beam width at the collector plane is equal to the source slit width multiplied with the magnification M of the instrument, a parameter defined by the geometry of the magnet that is usually around 1.

Since also the sum of aberrations A of the system contributes to the beam size at the collector plane the resolution can be expressed as follows:

$$R = \frac{m}{\Delta m} = \frac{D_0}{s'' + |M|s' + \sum A} \tag{4.2.5}$$

For instance, in case of the *Element 2* ($M \sim 1$), the dispersion is about 140 mm. In order to achieve a resolution of 4000, a slit width of the entrance and the exit slit of about 17 μm is required.

4.3 Electric sector

Eqn (4.1.6) shows that the m/q value for a given radius is indirectly proportional to the accelerating voltage, or more precisely, to the kinetic energy of the ion. Thus, ions with the same mass, but with slightly different kinetic energies will be focused at different positions, which will result in peak broadening and a loss of resolution. In ICP-MS, the ions that reach the magnetic sector show a kinetic energy to which several factors have contributed. Usually ions have a kinetic energy which is directly related to the temperature of the plasma and which can be calculated by the Boltzmann equation. Additionally, ions are generated in the plasma at a potential different from the potential of the interface and additionally, in the interface the ions are all accelerated by gas dynamics to the same velocity of the argon gas flow. This means that the kinetic energy increases proportional to the mass of the ion. All these factors contribute to the final ion kinetic energies and can affect the resolution of the magnetic device. This is the reason why a device is needed by which differences in energy can be compensated for. In most instruments, an electric sector is used for this purpose. Only in one type of instrument (*IsoProbe*), collisional cooling and focusing is accomplished by collision with a buffer gas in an rf-mutipole cell.

For a particle, with charge q, mass m and velocity v, injected into an electric field produced by a cylindrical condenser at a radius r_e, the centrifugal force of motion (left hand side of eqn (4.3.1)) must be equal to the centripetal force of the electric field

$$\frac{mv^2}{r_e} = qE \tag{4.3.1}$$

The kinetic energy (right hand side of eqn (4.3.2).) of a particle accelerated in an electric field is

$$qU_0 = \frac{1}{2}mv^2 \quad (4.3.2)$$

Thus the velocity can be calculated by

$$v = \sqrt{\frac{2qU_0}{m}} \quad (4.3.3)$$

And combining with eqn (4.3.1)

$$\frac{2mqU_0}{r_e m} = qE \quad (4.3.4)$$

$$\frac{2U_0}{r_e} = E \quad (4.3.5)$$

$$r_e = \frac{2U_0}{E} \quad (4.3.6)$$

This equation is similar to eqn (4.1.5), but does not contain the mass of the ion and thus, the electric sector does not have any mass dispersion. If a slit is placed at a particular position behind the system at the radius r_e, the system acts as an energy filter. (It should be mentioned here that due to the very low energy spread, *e.g.*, in thermal ionization these instruments typically don't require an electric sector.)

4.4 Double-focusing conditions

Summarizing so far, we know that the magnetic sector is a dispersive ion optical element with respect to mass and energy (momentum) and the electric sector is a dispersive ion optical element with respect to energy only. Both systems provide angular focusing properties. This means that an ion beam with a certain angular divergence is focused at an image plane. If the energy dispersion of the magnet ${}^{m}D_E$ and of the electric sector ${}^{e}D_E$ are equal in magnitude, but of opposite direction, magnet and electric sector (or sometimes named electrostatic analyzer – ESA), focus both ion angles (first focusing) and ion energies (double-focusing), while being dispersive for m/q only. This is the reason why devices which consist of an electric and magnetic sector fulfilling the following requirement (e: electric; m: magnetic)

$${}^{e}D_E + {}^{m}D_E = 0 \quad (4.4.1)$$

are termed "double-focusing" instruments.

Only for some well-defined combinations of electric and magnetic sector angles, the directional (angular) focus coincides with the energy focus.

In general, eqn (4.4.1) can become very complicated even for a basic design. This should be discussed here by means of the well known Nier–Johnson geometry. The parameters and angles are explained in Fig. 8.

The energy dispersion for a homogenous magnetic sector of a total angle ϕ_m is given as

$${}^{m}D_E = \frac{r_m}{2}\left(1 - \cos\phi_m + \frac{l'_m}{r_m}\sin\phi_m\right) \quad (4.4.2)$$

And the energy dispersion for a homogenous cylindrical electric sector of a total angle ϕ_e is given as

$${}^{e}D_E = \frac{r_e}{2}\left[\left(1 - \cos\sqrt{2}\phi_e\right) + \frac{l''_e}{r_e}\sqrt{2}\sin\sqrt{2}\phi_e\right] \quad (4.4.3)$$

Using the double-focusing condition of eqn (4.4.1) this equation results in:

$$r_e\left(1 - \cos\sqrt{2}\phi_e\right) + l''_e\sqrt{2}\sin\sqrt{2}\phi_e + r_m(1 - \cos\phi_m) + l'_m\sin\phi_m = 0 \quad (4.4.4)$$

Using eqn (4.1.2) for r_m it can be recognized that the equation is mass dependant and thus the double-focusing conditions is valid only for a single mass focused at the exit slit. As a consequence, such geometry is very well suited for a single collector arrangement operated in a scanning mode.

Fig. 8 shows the geometry of a multi-collector arrangement in a forward Nier–Johnson geometry. This arrangement is based on the fact that the double-focusing conditions are fulfilled on a curved graph to which the collector arrangement is fitted.

Eqn (4.4.4). looks rather difficult for most geometries, but can become very simple in case of the Mattauch–Herzog geometry which is shown in Fig. 9.

For this geometry the magnetic and electric sector are given in the following way:

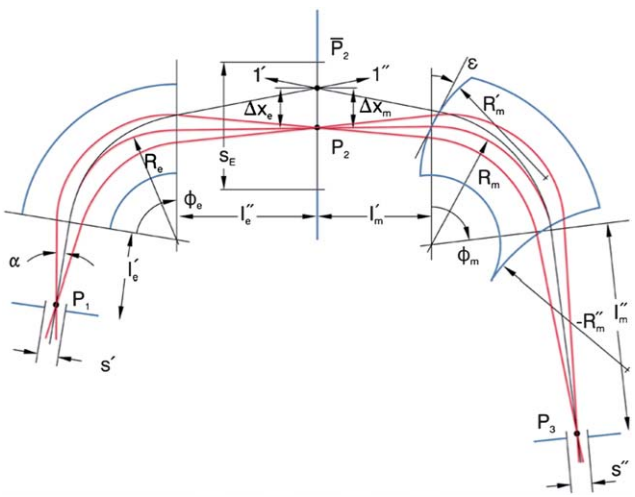

Fig. 8 Schematic of a forward Nier–Johnson geometry.

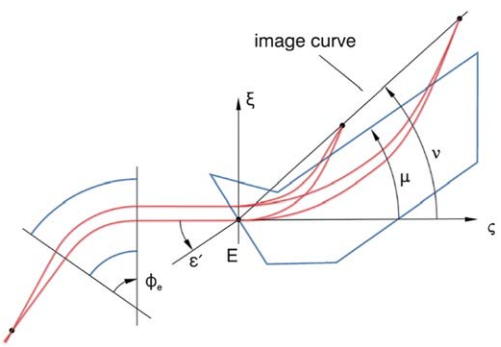

Fig. 9 Schematic of a Mattauch–Herzog geometry.

$$\phi_m = 90^\circ$$
$$\phi_e = \frac{\pi}{4\sqrt{2}} = 31.8^\circ$$
$$\varepsilon' = 0 \qquad (4.4.5a\text{–}f)$$
$$\varepsilon'' = -45^\circ$$
$$l''_e \to \infty$$

For all masses, the foci are located on a plane and thus this geometry is perfectly suited for simultaneous detection and found widespread applications with photo plates for ion detection in SSMS. Nowadays, instruments with such a set-up are commercially available under the form of transportable gas analyzers with an electronic focal plane camera (for details please visit http://www.oico.com). As has been mentioned previously, prototype GD- and ICP-MS instruments relying on the Mattauch–Herzog geometry have been developed in Gary Hieftje's group and recently, Spectro Analytical Instruments GmbH, Kleve, Germany, launched an instrument based on this geometry to the market (see section 5.2.2.5).[132]

5 Instrumentation

5.1 Components of a sector field instrument

All ICP/GD sector field instruments consist of

- an ion source,
- a sampling interface,
- an electrostatic lens system,
- a magnetic sector,
- an electric sector (or a collision cell),
- a flight tube,
- an entrance and a(n) collector (exit) slit, the combination which defines the resolution,
- transfer, zoom and/or filter optics,
- a detection system and
- a vacuum system

5.1.1 Plasma ion sources. Plasma-based sector field instruments are commercially available with an inductively coupled plasma (ICP) or a glow discharge (GD) plasma ion source. The source has an impact on the front end design only and will be discussed briefly in the following sections.

5.1.1.1 Inductively coupled plasma (ICP) source. ICP sources have a similar design in all commercially available instruments, independent on the type of mass separator (*e.g.*, sector field, quadrupole, time-of-flight) used. The ICP is generated according to an electrodeless approach in a discharge gas (usually argon) by application of a high frequency electrical current to an induction coil, which results in electromagnetic induction by a time-varying magnetic field. The coil is located around a torch and usually consists of 2 or 3 turns of copper tube, that is cooled with either water or Ar. The torch itself consists of three concentric tubes. The outer tube carries the cool or plasma gas (typically 13–15 L min^{-1}), which is responsible for the main supply of Ar to the plasma. The cool gas also helps to stabilise the plasma and finally cools the outer glass jacket of the torch. All tubes are made of fused silicate glass or quartz. The middle tube provides the auxiliary gas (0.5–2 L min^{-1}). The role of the auxiliary gas is to lift the plasma off the injector. The cool and auxiliary gases are injected tangentially in order to create a vortex and stabilise the plasma. The Fassel torch (most commonly used torch design) is designed to produce a stable toroidal plasma through the centre of which the sample aerosol (sample, carrier or nebulizer gas 0.8–1 L min^{-1}) is injected. After external ignition by a spark, an oscillating magnetic field is developed around the coil, which in turn, induces a high frequency oscillating electron and ion current, by which the plasma gas is heated to high temperatures (gas-kinetic temperature of 5000–8000 K, ionization temperature about 7500 K, excitation temperature 6500–7000 K, and electron temperature about 10 000 K).

The ICP is thus maintained by inductive heating. The electrical power applied ranges typically between 1000 and 1500 W, which is much higher than the typical value of 100 W for a glow discharge. Ranges from 500–800 W are usually applied when cold plasma conditions are accomplished.

The aerosol which is generated from the sample (created most often by nebulisation of a liquid sample solution or consisting of solid particles carried by a gas flow when sample material is ablated by a laser) is transferred into the centre of the plasma by an Ar gas flow. The temperature in this plasma is sufficiently high to give rise to efficient volatilization and atomization of the sample components and subsequent excitation and ionization of the atoms thus formed. Predominantly singly charged ions are generated for all elements of the periodic table. The ionization efficiency calculated from the Saha–Eggert Equation[133] by using the electron densities and temperatures typical for the ICP discharge show that all elements with first ionization potentials below 8 eV are completely (>90%) ionized and even elements with first ionization potentials between 8 and 12 eV are ionized by more than 10%. Thus, the mass spectrum observed mainly consists of signals corresponding to the singly charged elemental ions of the nuclides of all elements present in the sample.

The plasma is generated in a torch arrangement and for some instruments, this torch is equipped with a guard electrode (GE) or plasma shield, which is a grounded metal plate placed in-between the plasma torch and the load coil. This device decreases the ion energy spread, and thus can help to increase the overall ion transmission of a sector field device. For some instruments (*e.g.*, the *Element 2*), the GE is in particular required for cold plasma to prevent secondary discharges between the ICP and the grounded interface.

5.1.1.2 Glow discharge source. Glow discharge plasmas are the simplest to generate. In its simplest form, a glow discharge plasma is created by applying a dc potential difference (on the order of 500 to 1500 V) between two electrodes (anode and cathode), which are inserted in a container filled with a (noble) gas, most often at a reduced pressure. Depending on the distance between the electrodes, different plasma forms are established and one of these plasmas closest to the cathode was given the name glow discharge because of the emission of glowing light.

This plasma is generated by fast electrons emitted from the cathode, ionizing and exciting the noble gas atoms. Ions from the plasma that are close to the cathode (which is the sample to be analyzed) are accelerated towards the cathode, where they sputter the electrode material and produce those fast electrons which are needed to sustain the discharge. The neutral atoms sputtered from the electrode material diffuse into the glow

discharge plasma, where they can become excited or ionized. Conducting materials, such as metals, alloys and semi-conductors, can be used as cathode material and thus, be analyzed by either emission or mass spectrometry.

For typical analytical applications (such as mass spectrometry or optical emission spectrometry), the gas is usually argon (or sometimes neon) and the gas pressure is set typically in the range 50–700 Pa. Because the processes of sputtering and ionization are separated, minimal non-spectral matrix effects are expected. More details can be found in text books[134,135] and in the literature[136,137] and selected applications will be discussed in part II.

5.1.2 Sampling interface. The sampling interface is a crucial and non-trivial part of the mass spectrometer and has to transfer ions from the plasma, which is operated at ambient pressure in the case of ICP or at a few hundred Pa in the case of GD, to the mass analyzer, which is operated under vacuum (see section 5.1.8). The interface design is thus very similar to those of quadrupole-based instruments, even if it is operated for some instruments at high voltage to provide the ion acceleration (and thus increase the kinetic energy of the ions) as needed for operation.

The interface of an ICP ion source is usually water-cooled and made of materials with good thermal conductivity. It holds the sampler and skimmer cones, which are in general hat-shaped metal plates with a small orifice (0.4–1.2 mm) in the centre in order to sample the centre part of the ion beam generated in the plasma. The diameter of the orifice has to be large enough to allow maximum transmission and reduce clogging, whereas the vacuum still has to be maintained. The skimmer cone is in general sharper and has a smaller orifice than the sampler cone. The cones are placed co-axially at a short distance (several mm) from one another, allowing a sequential pressure decrease. Shape, material and orifice diameter can have an impact on the instrumental performance in terms of, *e.g.*, transmission efficiency or formation of interfering polyatomic ions. The cones are usually made of Ni, even though Pt covered cones are preferable for low Ni blank level or for analyzing very corrosive solutions. For laser ablation purposes, cones manufactured from Al are used, as well. In order to reduce effects of electrostatic coupling between the load coil and the plasma discharge, resulting in an electrical discharge between plasma and sampler cone, the load coil is usually grounded at the side facing the sampler cone.

In case of a GD plasma ion source, usually only one cone is needed, because the pressure in the ion source is already reduced to a few hundred Pa. A roughing pump is used for differential pumping in both ion source arrangements.

The ions from the ICP or GD source are accelerated after passing the interface region. An acceleration voltage ranging from 4000 to 10 000 V – depending on the particular instrument – is applied behind the interface. There are two possibilities: a) the ICP and interface are at high potential and the analyzer at ground potential or b) the ICP and the interface are at ground potential and the mass analyzer is floating at high potential. Due to the curved shape of sector field devices, no additional means (*e.g.*, photon or shadow stop or ion mirror) are required to hinder neutrals and photons generated in the plasma from reaching the detector. Whereas a neutral 'cloud' of ions and electrons can be observed within the interface region, the electrons diffuse much quicker in the high vacuum region after the skimmer cone. Together with a first lens displaying a potential more negative than that of the ICP, this is resulting in a positively charged ion beam, which is further guided and shaped by a series of electrostatic lenses.

5.1.3 Lens system. The lens system is used to guide, focus and accelerate the positively charged ion beam onto the entrance slit and to shape the circular peak profile of the ion beam behind the skimmer to a more rectangular (in reality eliptical) profile in accordance to the geometry of the entrance slit. Therefore, the lens system is more complex in a sector field device than in a quadrupole-based instrument. It consists of number of electrostatic lenses (cylindrical and quadrupole). An extraction lens is usually placed directly behind the skimmer cone to attract and accelerate ions leaving the extraction chamber *via* the skimmer cone aperture. In comparison to quadrupole instruments much higher acceleration voltages are used and this is one of the reasons why sector field instruments show a higher transmission of low mass elements and a more uniform response throughout the mass range. In some instruments, the ion beam is accelerated in this lens system to the full acceleration voltage (*e.g.*, ~8000 V for the *Element 2*). Sector field instruments provide the possibility of electric mass scanning or *E*-scanning by means of adapting the acceleration voltage (see section 6.).

In common with most ion optical focusing devices, a magnetic sector mass spectrometer typically has some significant aberrations which are, among other, function of the angular spread of the ion beam. To obtain a high resolving power and to reduce transmission losses, these aberrations must be kept below certain limits. The angular divergence α of the ion beam is inversely proportional to the square root of the accelerating voltage.

$$\alpha \propto \frac{1}{\sqrt{U_0}} \tag{5.1.1}$$

Therefore, it is usually preferred to apply a high acceleration voltage, which usually is limited only by practical and economical factors.

5.1.4 Magnetic sector. The magnetic field disperses ions according to their mass and energy (momentum). Single collector ICP-SFMS instruments require an electromagnet with minimized hysteresis because of the need to scan the magnet. Therefore, laminated magnets are used in different shapes or geometries (see description of the instruments). Moreover, (water) cooling of the magnet coils is a prerequisite for highest mass stability. When using MC-devices with Nier–Johnson geometry for isotope ratio measurements, the magnet is typically operated at a constant field (static mode). Nevertheless, also these devices require a laminated magnet with minimum hysteresis, (i) because the magnet settings need to be changed when defining another mass range, containing the isotopes to be measured, and, thus also, (ii) for allowing dynamic operation (wherein a change of the magnetic field is required during the isotope ratio measurements) in MC-ICP-SFMS. The field strength of the electromagnet can be changed by alternating the electric current at the coils usually made of copper wires. The magnetic field is controlled by a magnetic field regulator with a high power stage, which allows a very fast scan speed and provides an extremely stable field.

The Mattauch–Herzog geometry does not require a change in the magnetic field as it is operated in full static mode and all ions are focused on one focal plane without scanning. Therefore, this instrument does not require an electromagnet and thus can be equipped with a (cheaper) permanent magnet of constant field strength instead.

5.1.5 Electric sector. In the electric sector, differences in ion energies are compensated for to a certain extent. A spread in the ion energy limits the mass resolution attainable. The energy spread of ions originating from the ICP plasma can be up to 20 electron volts (eV), thus requiring an electric sector in order to achieve high resolution capabilities. The energy spread can already be reduced significantly down to a few eV by applying a shield at the ICP source. It should be mentioned here that this energy spread is more pronounced for ions coming from an ICP ion source than for those produced in a GD source.

As has been mentioned before, the combination of radius and angle of the magnetic and electric sectors need to fulfil certain conditions to guarantee double-focusing conditions, either for a single mass (or slit for single collector devices) or on a well-defined curve (on which the Faraday cups are located in a multi-collector device). Small magnets typically require small electric sectors as well, the smallest being 105 mm only in the *Element 2*, whereas the largest can go up to 943 mm with an angle of 70° in case of the *Nu Plasma 1700*. Cylindrical or toroidal geometries of the electric condenser electrodes are typically chosen.

As alternative approach, the *IsoProbe* has only one (magnetic) sector and the energy spread is reduced by means of a collision cell. As this instrument is no longer commercially available, the literature is referred to for more details.[11]

5.1.6 Slit system. The slit system is required in order to shape the geometry of the ion beam. Moreover, the resolution depends on the width of the incident ion beam, which is defined by the width of the entrance (alpha or source defining) slit. After passing through the entrance slit, the ions are injected perpendicular to the magnetic field and traverse the field on different circular trajectories, according to their mass/charge ratio. The image of the entrance slit is focused onto a second (exit, collector or imaging) slit. Decreasing the source (and/or collector slit widths) can be used to increase mass resolution. Full high resolution spectra are accomplished when decreasing the slit width of both entrance and exit slit simultaneously, whereas multiple collector devices are typically operated in pseudo-high resolution mode, using the entrance slit only. The interference is clipped away on the slit infront of the detector. More details on the operation principle are given in sections 6.1.2 and 6.2. Finally, it has to be considered that the continuous bombardment of the entrance slit with ions of keV energies leads to a continuous sputtering of material. Even though the sputtered material is not detected during operation (as generated ions do not show the correct energy, required to pass through the mass analyzer), it leads to a continuous degradation of the slit geometry and results in a deterioration of the beam profile. The consequences hereof are loss of resolution and degradation of the peak profile and increased abundance sensitivity. Therefore, slit systems have to be exchanged regularly.

5.1.7 Zoom lens and energy filter. After mass separation is accomplished, multi-collector devices use ion optical systems in order to maintain the direct guidance of the incoming ion beams into the detector. The corresponding optics are generally referred to as 'zoom lens' or 'zoom optics' as is it is used to magnify or demagnify the ion beam image. Two different setups of zoom optics will be discussed (for the *Neptune Plus* and the *Nu Plasma II*, respectively). (see section 5.2.2.1).

In order to improve abundance sensitivity (see section 3.6), special energy filters, permitting ions with sufficiently high kinetic energies to pass only, are sometimes applied in sector field devices.

5.1.8 Detectors. The detection systems of single collector sector field instruments are similar to those in other ICP-MS instruments. All commercially available single collector instruments are equipped with an electron multiplier (discrete dynode detector), which can be operated in analogue and counting mode, thus allowing to cope with a large variation in the number of incident ions. In some cases, an additional Faraday cup is available for measuring higher intensities, expanding the linear dynamic range by about three to four orders of magnitude (instrumental details see section 5.2).

Multi-collector devices use a number of Faraday detectors which are arranged along the focal plane to measure all isotopes of interest simultaneously, which is a prerequisite for optimum isotope ratio precision. In addition to Faraday cups, electron multipliers, including both discrete dynode detectors and Channeltrons are used for the monitoring of nuclides with low isotopic abundance or at low analyte concentration (instrumental details, see section 5.2). A detailed description of detectors can be found elsewhere.[138]

5.1.9 Vacuum system including flight tube. A peculiarity of sector field mass analysers is the curved flight tube, which is located between the poles of the electromagnet. The vacuum system of a sector field instrument is of crucial importance since the high kinetic energy and the longer flight path (compared to quadrupole-based instruments) would otherwise lead to a significant scatter of ions, loss of transmission and deteriorated abundance sensitivity.

As an ICP is operated at ambient pressure, differential pumping systems are used to decrease the pressure (plasma: about 100 000 Pa – interface: 10–500 Pa – analyzer: 10^{-6} to 10^{-7} Pa) and thus, ensure maximum transmission efficiency of the ions is achieved. The interface region is pumped by a regular rotary pump. As the sampler cone provides a permanent aperture between ambient atmosphere and the high vacuum part, the mass analyzer can be separated from the interface region *via* a slide valve, which is located usually directly behind the skimmer cone. This valve is only opened when the plasma is operating stable and is closed before plasma shutdown. Therefore, the pumping of the interface is only required if the plasma is in operation. As a consequence, the interface pump is operating separately from the high vacuum system. A higher amount of corrosive gases can be found in the interface region, which is pumped by the interface pump. Therefore, the oil of the interface pump requires a regular change. The vacuum which is obtained by the interface pump has an impact on the instrumental performance features, such as transmission

efficiency or abundance sensitivity. As a consequence, stronger vacuum pumps are becoming popular in ICP-SFMS systems.

The lens system is usually operated in a medium vacuum range (10^{-3} Pa), whereas the analyser must be operated under higher (compared to a quadrupole-based instrument) vacuum conditions ($\sim 10^{-5}$ Pa). The vacuum required is achieved by using a differential pumping system (vane-type rotary pump in combination with turbo-molecular pumps). An even higher vacuum has proven advantageous in the case of multi-collector devices. Multi-collector instruments use additional ion getter pumps in order to provide a vacuum down to 10^{-7} Pa in the analyzer part of the instrument. The analyzer part can be separated by an additional valve from the lens system.

5.2 Commercially available instruments

Over the years, the significant reduction in cost has led to a noticeable increase in number of sector field instruments, which now account for almost 10% of all ICP-MS instruments worldwide. Table 1 gives an overview of instruments which have been launched onto the market.

In the following section, we provide more detailed information on sector field instruments which are currently commercially available.

The *Element series* (*Element*, *Element 2 and Element XR*) (Thermo Fisher Scientific, Bremen, Germany) is the most widespread commercially available single-collector ICP-SFMS. Nu Instruments (Wrexham, UK) introduced the *AttoM* in 2004. The three multi-collector instruments currently available are the *Neptune plus* (*an improved version of the Neptune*) (Thermo Fisher Scientific) and the *Nu Plasma II* (Nu Instruments) and the *Nu Plasma 1700* (Nu Instruments). In January 2010, a new sector field device with Mattauch–Herzog geometry came to the market, the *Spectro MS* (Spectro, Germany).

For completeness, it should be mentioned that older instruments that are no longer produced are still in use and some applications carried out with these types of units are partially covered in part II of this series of review papers. This holds true for the first multi-collector instruments, including the *Plasma 54* (VG Elemental), the *Axiom* (Thermo Optek) and the *IsoProbe* (GV Instruments) and single collector ICP-SFMS, including

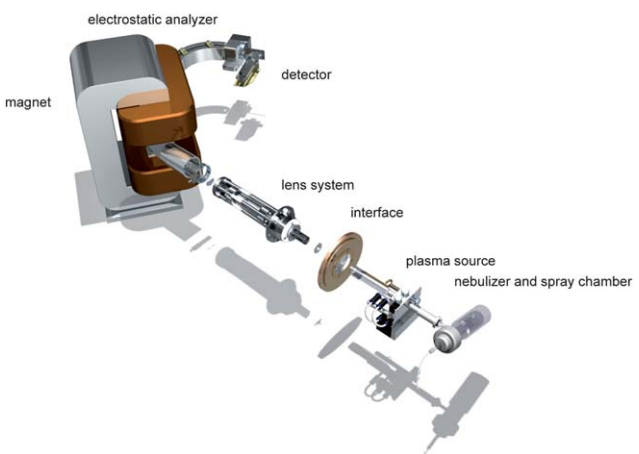

Fig. 10 Schematic drawing of the *Element 2* (*Thermo Fisher Scientific*).

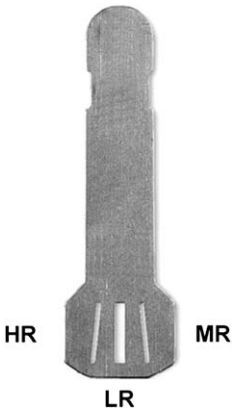

Fig. 11 Slit holder of the *Element 2* (*Thermo Fisher Scientific*).

Plasmax and *Plasmax* 2 (Jeol), the Axiom (Thermo Optek), the *PlasmaTrace 2* (Micromass) and the *Element* (Thermo Fisher Scientific). These instruments will not be discussed in more detail here.

5.2.1 Single collector instruments

5.2.1.1 Element 2 and XR. The ICP-SFMS instruments *Element 2* and *XR* (Thermo Fisher Scientific) both evolved from the *Element* and thus share a number of hardware components. They have a small magnetic sector with a radius of only 16 cm, followed by a 10.5 cm radius toroidal electrostatic sector in a reverse Nier–Johnson geometry. The whole mass analyzer, including the lens system, the flight tube and also the electric sector is operated at a high potential of about 8 kV and thus, the interface is kept at ground potential, allowing to keep the interface pumps at ground potential and providing easy coupling of different inlet devices.

A schematic sketch of the *Element 2* is shown in Fig. 10. The slit system of the *Element 2* and *Element XR*, consists of three fixed slits arranged on one single holder (Fig. 11). The slit width for a resolution of ~10 000 is about 5 μm only, increasing to 16 μm for a resolution of ~4000. In the low resolution mode (R ~300) flat top peaks are achieved. The slit holder is operated pneumatically under computer control and functions like a pendulum which can swing to the left and right hand side, thus switching reliably between low (LR), medium (MR) and high (HR) mass resolution within less than one second. Recently, the precision for isotopic analysis of chromium (RSD for $^{53}Cr/^{52}Cr$: 0.005% at 1 ppb) and sulfur (RSD for $^{34}S/^{32}S$: 0.01% for 100 ppb IRMM-643) could be improved with the *Element 2* and *Element XR* by using flat top peaks at a resolution of about 2500, as obtained with a built-for-purpose slit.

A single secondary electron multiplier can be operated in a combination of 'analogue' and 'counting' modes to provide a linear dynamic range of ~9 orders of magnitude. Both detection modes are "cross-calibrated" automatically. The dark noise measured with the instrument is below 0.2 cps and the sensitivity achieved with a standard inlet system is more than 1×10^9 cps/ppm (measured at a mass resolution of 300 for a solution containing indium at a concentration of 1 μg mL^{-1}). With the new introduced "Jet Interface" option, the sensitivity for indium is even more than 2×10^{10} cps/ppm under the same conditions.

In the *Element GD* and *Element XR*, an extended dynamic range of more than 12 orders of magnitude is provided by addition of a Faraday cup with a fast amplifier. In the Faraday mode, integration times down to a millisecond are achieved when going from high sensitivities to low or *vice versa*. Such a large dynamic range, exceeding that of quadrupole-based instruments significantly, is useful to measure matrix components in one run together with the ultra-trace elements, *e.g.*, in laser ablation analysis. To improve the abundance sensitivity, the *Element XR* has an retardation filter lens, *e.g.*, allowing the determination of extreme isotope ratios. The example in Fig. 12 shows the effect of the retardation lens on the signal for the minor Th isotope ^{230}Th. The standard used is IRMM-036 with a ratio of ^{230}Th/^{232}Th = 3.11 ppm. By using the filter lens, the peak tail of the intense ^{232}Th peak is no longer contributing at ^{230}Th. For these measurements, a new slit combination was used that allows flat top peaks at a resolution of ~2500.

5.2.1.2 Element GD. Thermo Fisher Scientific introduced a GD-SFMS instrument, the *Element GD*, in 2005. The *Element GD* combines a new fast flow dc GD ion source (see picture and schematic representation in Fig. 13a,b) with the mass analyzer from the *Element 2* ICP-SFMS instrument. The anode and the cathode plate of the source are separated by an insulator. The flat sample is pressed by a holder against the cathode body. Sample cooling is provided to the anode plate by means of a Peltier cooling device. In this source, a flow tube is used to direct the gas flow perpendicular to the sample surface and by application of high flow rates, the ion transport towards the sampling orifice is improved. Gas flow rates of a few hundred mL min^{-1} are used, resulting in discharge powers of up to 100 W.

Fig. 14 is a picture of a Cu sample after sputtering, which clearly shows the glow discharge sputter crater with as diameter of 8 mm. Sensitivities of more than 10^{10} cps (1.6×10^{-9} A as peak height) are achieved for a copper matrix measured at medium mass resolution ($R \sim 4000$).[139] Analytical applications with this device are presented in part II.

By incorporation of a Faraday cup into the ion detection module (the same design as used in the *Element XR*), this instrument covers a dynamic range of more than 12 orders of magnitude. This is essential for bulk analysis, where the signal intensities for the measured trace elements are always related to the matrix ion intensity, serving as internal standard to overcome possible drift effects, as well as to perform quantification *via*

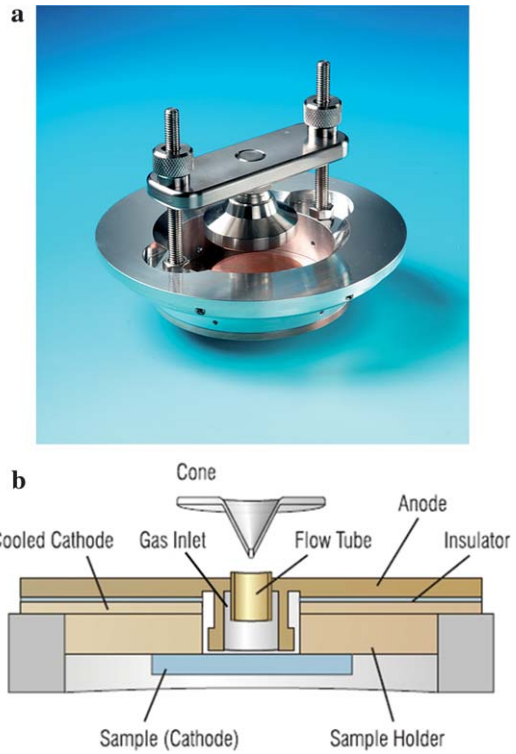

Fig. 13 (a) Photo of the GD sample holder of the *Element GD* (*Thermo Fisher Scientific*) showing the sample holder and the cathode body. The metallic sample is pressed against the cathode body by the sample holder. (b) Schematic of the ff-GD ion source of the *Element GD* (*Thermo Fisher Scientific*) *which consists of two electrodes*: *a cathode with the sample and an anode. A* flow tube the argon gas flow is directed onto the surface of the metallic sample. A cone, very similar to the skimmer cone of an ICP-MS is used to extract the ions from the GD source.

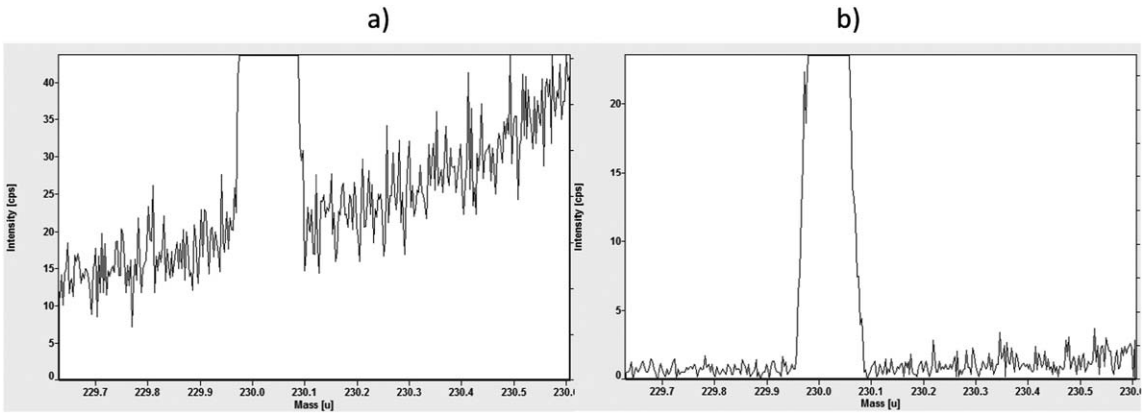

Fig. 12 Illustration of improved abundance sensitivity offered by the filter lens, which only transmits ions with appropriate kinetic energy – measurement of the Th isotope ^{230}Th in the standard IRMM-036 by means of an *Element XR* (Thermo Scientific): (a) without filter lens, the ^{230}Th signal is superimposed on "the wing" of the much more intense ^{232}Th signal, (b) with filter lens, on the other hand, the signal intensities in the vicinity of the ^{230}Th peak are reduced to normal background levels.

Fig. 14 Crater from 3 different sputtering events in the GD source of the *Element GD* (*sample*: *BCR copper standard CRM 075*).

relative sensitivity factors (RSFs).[140] Except for the ion source and the interface flange, most of the other hardware and software features are similar to those of the *Element 2*/*XR*.

5.2.1.3 AttoM. The *AttoM* (Nu Instruments) is a double-focusing, high resolution ICP sector field mass spectrometer from Nu Instruments and was introduced to the market in 2004. The mass analyzer consists of a 320 mm radius ESA and a 250 mm radius magnet in Nier–Johnson geometry. A schematic representation of the instrument is provided in Fig. 15 The interface and the fore pump are floating at a potential of 6 kV, whereas the analyzer is at ground potential. The *AttoM* uses 3 variable computer controlled slit assemblies to provide resolutions from 300 to >10 000. Besides entrance and exit slit, the

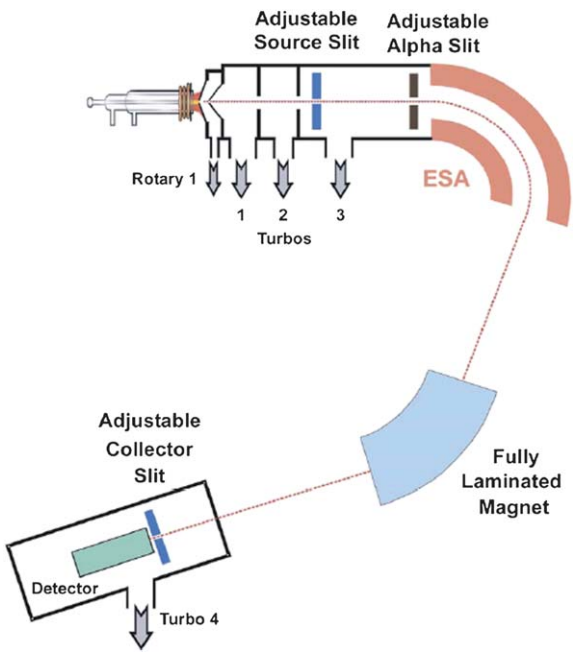

Fig. 15 Schematic drawing of the *Nu AttoM* (*Nu Instruments*) (source: Nu Instruments).

AttoM has an additional Alpha slit in front of the ESA in order to correct for beam aberrations and to limit the energy spread. A single secondary electron multiplier provides a linear dynamic range of 9 orders of magnitude. In contrast to the *Element 2*, this is achieved by ion beam attenuation in the lens system, and thus no cross-calibration between the analogue and counting modes is required. Also here, an extended dynamic range of up to 12 orders of magnitude is provided by an additional Faraday cup with a fast amplifier. In order to avoid mass discrimination effects introduced by a change of the acceleration voltage, the *Nu AttoM* incorporates an ion optics system which allows alteration of the ion trajectories within the magnet. This offers the advantage of beam deflection at constant acceleration energy and ESA voltages and therefore, avoiding additional mass discrimination effects (see section 6.3). By applying different voltages to the lens assembly, the entrance angle of the ion beam is altered, such that its trajectory is changed. An ion beam of a certain mass can therefore be deflected either to a lower or higher "apparent" mass. A mass range of up to 40% of a given mass can be covered in that way. This feature is also used in combination with the fast magnetic scanning to increase the integration time for selected nuclides during elemental analysis along the whole mass range (see section 6.1.1).

5.2.1.4 Astrum. The *Astrum* (Nu Instruments) is a double-focusing, high resolution GD sector field mass spectrometer, based on the hardware of the *Nu AttoM* ICP-SFMS instrument and was introduced in 2010. At the time of writing, there are no installations. The glow discharge source is based on a low pressure static discharge and consists of a tantalum cell allowing both pin and flat sample configurations. A cryogenic cooling option allows analysis of samples with low melting points. The combination of an electron multiplier and a Faraday detector enables a linear dynamic range of 12 orders of magnitude, enabling monitoring of matrix and trace elements in a single scan. The hardware configuration of the mass spectrometer is that of the *AttoM* ICP-SFMS.

5.2.2 Multi-collector ICP-MS instruments. Since the introduction of the first MC-ICP-SFMS system in 1992 (the *Plasma 54* from VG Elemental), more than 225 MC-ICP-SFMS units have been installed in about 200 different laboratories worldwide. The initial hope for MC-ICP-SFMS was that it would simplify measurements normally carried out *via* thermal ionization mass spectrometry (TIMS) (*e.g.*, Pb, Sr, Nd, U, Th, Pu, Os) by marrying the favourable ionization characteristics of an ICP source with the high isotope ratio precision required in many applications. Such a high precision can be attained with a multi-collector array in order to eliminate the problems encountered with sequential scanning and plasma flicker in isotope ratio measurements (for more details see ref. 141). Even though more and more MC-ICP-MS are used for 'traditional' TIMS applications, both instruments have their (often complementary) importance in isotope ratio analysis.

5.2.2.1 Nu Plasma II. The *Nu Plasma II* (Nu Instruments) was launched in 2010 and is the enhanced version of the *Nu Plasma* (launched in 1997). The instrument consists of a 350 mm radius ESA and 250 mm radius magnet in Nier–Johnson

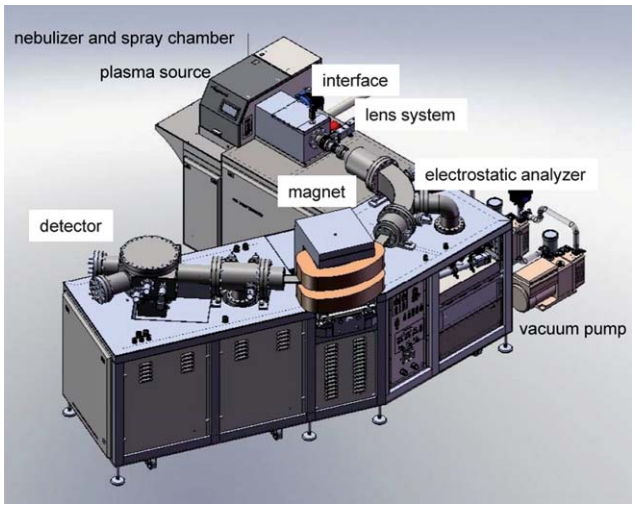

Fig. 16 Schematic drawing of *Nu Plasma II* (*Nu Instruments*) (source: Nu Instruments).

geometry. Interface and fore pump are floating at a potential of 6 kV, whereas the analyzer is at ground potential. The schematic drawing of the instrument is given in Fig. 16.

The lens system of this instrument is shown in Fig. 17. The *Nu Plasma II* MC-ICP-SFMS has a pre-selectable entrance (source) slit system for three resolutions with slit widths of 30, 50 and 300 μm. The slits are mechanically moved into the ion beam *via* linear drive. An additional α-slit is placed between source slit and ESA entrance and is fully adjustable from 0 to 7 mm by computer control. Basically, the α-slit reduces beam aberrations caused by a diverging beam entering the magnet, producing a blurred image at the collector. In case full resolution spectra are required, a moveable slit can be moved mechanically in front of the detector grid in order to reduce the entrance widths to the cups from 1 to 0 mm. This is only possible since the detectors are in a fixed position. Mass resolutions settings of 300 to >7000 can be achieved (10% valley definition).

The detector array consists of 16 Faraday cup detectors at fixed positions. The steering of the ions into the cups is accomplished *via* variable zoom optics by which the mechanical complexity of the detector array is significantly reduced. The *Nu Plasma II* has a dispersion of about 500 mm, leading to a separation of, *e.g.*, the Pb isotopes of about 2.5 mm, which corresponds to the fixed separation of the detectors in the standard array. For heavier elements, magnification of the ion beam image is required for alignment into adjacent detectors. In contrast, for the lighter elements, a larger separation of the adjacent isotopes is obtained and therefore, the ion beam image has to be demagnified. However, the range of dispersion is limited without producing too much distortion. Therefore, isotopes of significantly lighter masses cannot be aligned into adjacent collectors, and every other collector or every third collector may have to be used instead. A number of variables can be altered for setting the zoom lens. These variables are provided by a database for each isotopic system of interest.

Within the Faraday collector array, up to five full size discrete dynode electron multipliers can be interspersed. A small double ESA assembly can deflect the two outer ion beams into off-axis secondary electron multipliers. The central beam passes through a slot in the central block. There is a small deflection imposed onto the ion beam to ensure that the multiplier does not lie directly in line with its central channel. This is necessary to deflect the ion beam if an intense signal is observed and also allows directing the ion beam to the first dynode of the multiplier. The same effect is achieved with the off-axis multipliers by slight altering of the deflection ESA voltages.

The *Nu Plasma II* can be equipped with a deceleration filter device which can be placed in front of each secondary electron multiplier. The application of the ion deceleration lens system in the Nu Plasma ICP-MS allowed, *e.g.*, a reduction of peak tailing from ^{238}U ions at $m/z = 236$ down to 3×10^{-9}, whereas the absolute sensitivity for uranium was reduced by only about 30%. Thus, abundance sensitivity was improved by almost two orders of magnitude and the minimum determinable ^{236}U/^{238}U ratio was

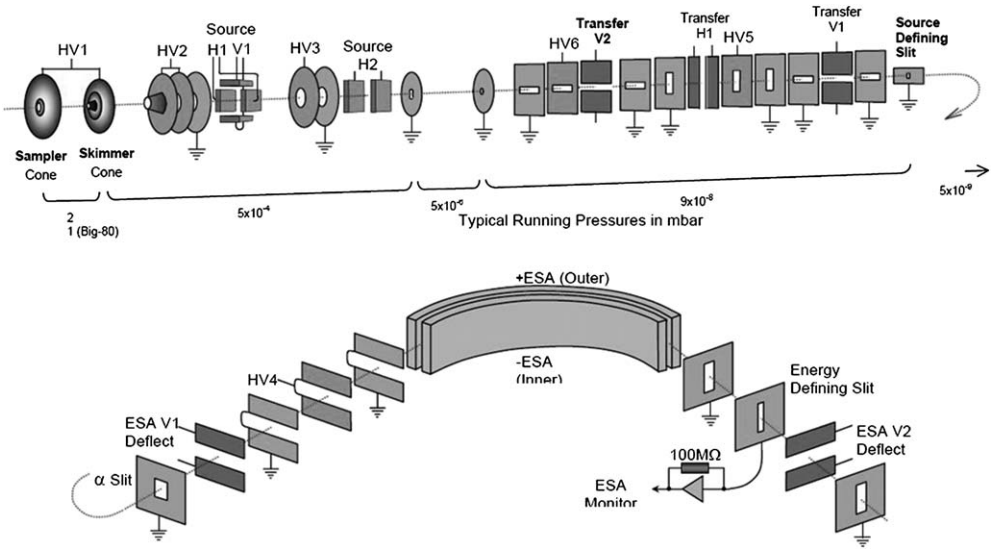

Fig. 17 Lens system of the *Nu Plasma II* (*Nu Instruments*) (source: Nu Instruments).

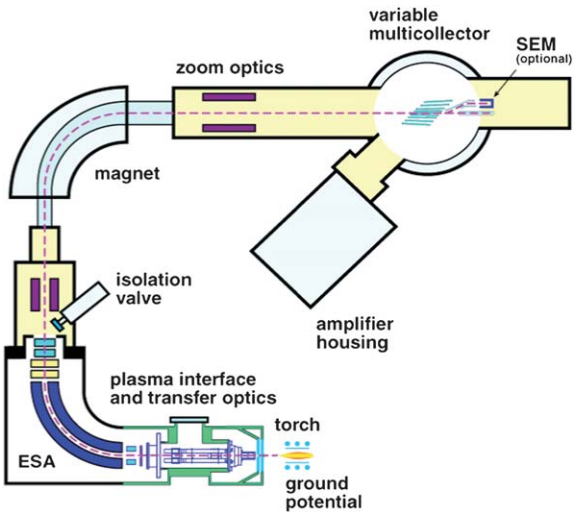

Fig. 18 Schematic drawing of the *Neptune* (*Thermo Fisher Scientific*).

improved by more than one order of magnitude compared with conventional sector-field ICP-MS or TIMS.[142]

5.2.2.2 Nu Plasma 1700. The large geometry of the *Nu Plasma 1700* (Nu Instruments) is used for high resolution isotope ratio measurements. The ion source is floated at 6 kV, whereas the analyzer is at ground potential. The instrument is designed with a high dispersion and large geometry and uses a single 750 mm radius, 70° magnet, combined with a 943 mm radius, 70° ESA, to provide a double-focusing arrangement. This assembly results in a mass dispersion of about 1760 mm, reflected in the instrument's name. Curved pole pieces and four multipole elements rotate the focal plane for right-angle intersection with the ion beams and ensure stigmatic focusing.

As opposed to other MC-ICP-SFMS instruments operated in pseudo high-resolution mode, *Nu Plasma 1700* simultaneously rejects interfering masses at both the low and high mass sides of the beams of interest. High-resolution tuning is achieved by means of a continuously adjustable source defining slit in combination with computer-controlled continuously adjustable collector slits at all 19 detectors. Aberration is minimized by selectable alpha restrictors and by higher-order functions applied to the four multipoles. With these provisions, the instrument achieves a resolving power up to 40 000 ($m/\Delta m$, 5% peak height) and maintains flat peak tops up to a mass resolution of 5000 (10% valley definition).

The *Nu Plasma 1700* has sixteen Faraday detectors, ten of which are incorporated in a fixed central array. The positions of the three detectors at the low mass side and the three at the high mass side are adjustable *via* a mechanical drive. The steering of the ions is accomplished *via* two quadrupole zoom lenses. The additional mechanical adjustment of the outer detectors is permitting simultaneous recording of ion beams of high dispersion. Three discrete-dynode electron multipliers, one of them equipped with a retardation filter, are interspersed with the fixed collector array.

5.2.2.3 Neptune *and* Neptune *plus.* The *Neptune* (Thermo Fisher Scientific, Bremen), has been commercially available since 2000 and is a double-focusing multi-collector ICP-MS instrument. It shares the ICP interface of the *Element 2* and the multi-collector technology of the TIMS instrument (*Triton*, Thermo Fisher Scientific) and combines high mass resolution, variable multi-collection, zoom optics and multiple ion counting (MIC). A mass dispersion of 812 mm provides space for the collector array. The mass dispersion is achieved by an ion optical magnification of 2. With increasing ion optical magnification, the divergence angles of the ion beams are reduced and the dispersion is increased. As a result, cups can be wider and deeper. Scattered particles released at the cup's side wall by the incoming ion beams are less likely to escape and do not alter the "true" ion current.

A schematic overview of the instrument is given in Fig. 18. The entrance slit system of the *Neptune* is designed like that of the *Element 2*. If required, special high resolution cups can be used, for which an exit slit is directly placed in front of that specific detector. Eight moveable collector supports and one fixed centre channel are installed on the optical bench of the high precision variable multi-collector module. The centre channel is equipped with a Faraday cup and optionally an ion counter, with or without a retardation lens (RPQ) to improve the abundance sensitivity. The eight detector supports where up to 17 collectors (9 faraday cups and 8 electron multipliers) can be mounted are motor-driven and can be precisely positioned along the focal plane, according to the specific needs of the application, and all of which can be used in a simultaneous multi-collector measurement. A position sensor is located beneath each variable detector platform inside the vacuum chamber to ensure reliable positioning.

The maximum distance between the outermost channels corresponds to a relative mass range of 17%, which is sufficient for the simultaneous measurement of ^{6}Li and ^{7}Li or for the range from ^{202}Hg to ^{238}U. Each moveable support can carry either a Faraday cup, or a miniature secondary electron multiplier (SEM), or a combination of both in a package. All detectors are of 'plug-in' design and can be readily exchanged. It is possible to equip one detector platform with a package of ion counters plus one Faraday cup. The above combination is applicable for specific elements in the high mass range, *e.g.*, lead and uranium, because the packages are very compact. The configuration where the ion counter packages are attached to the outer moveable Faraday cups maintains the full flexibility of the Faraday cup array as the insertion of the additional ion counters at these outer positions does not block any Faraday cup configuration.

The Faraday cups are laser machined from solid carbon to guarantee uniform response, high linearity, low noise and long lifetime. Each Faraday cup is connected to a current amplifier. The amplifier signal is digitized by a high linearity voltage-to-frequency converter with an equivalent digital resolution of 22 bits. This ensures sub-parts per million (ppm) digital resolution of all measured signals, independent of the actual signal intensity. The amplifiers are mounted in a doubly shielded, evacuated and thermostatic housing with a temperature stability of $\pm$ 0.01 °C. The dynamic range of the current amplifiers is extended to 50 V in positive ion detection mode. The extended dynamic range supports the measurement of large differences of the measured isotope ratios, and it directly leads to an improved signal-to-noise ratio for the minor isotopes.

An enhanced version of the *Neptune*, namely the *Neptune plus* was introduced in 2009.

Compared to the Neptune, new Compact Discrete Dynode multipliers (CDD) with the same performance as standard-sized discrete dynode multipliers enables simultaneous measurement of all U, Th and Pb isotopes in a multi-collector setup. The combination of a desolvation system and the "Jet Interface" also improves the sensitivity. The *Neptune plus* can also be equipped with the "Dual RPQ" option in order to, *e.g.*, improve the abundance sensitivity as required for adequate monitoring of the minor U isotopes.

5.2.2.4 Spectro MS. The main feature of multi-collector devices is the capability for simultaneous detection of all of the isotopes of interest by use of discrete detectors. Over the years, the number of Faraday cups in the collector array has been increased significantly and nowadays, it is possible to manufacture cups by micro-machining that are so small that all nuclides can be measured all the time for instance in a Mattauch–Herzog geometry (see also section 2.2.2).

A commercial Mattauch–Herzog instrument with an ICP ion source and a focal plane camera has been discussed last year at the Winter Conference on Plasma Spectrochemistry" in Fort Myers[143] and has been introduced to the market as the Spectro MS, a few weeks later at Pittcon by the company Spectro Analytical Instruments, Kleve, Germany, where it also was awarded for its innovative concept.[144] The instrument's core is a small Mattauch–Herzog mass spectrograph with a 120 mm focal plane permanent magnet, onto which a 120 mm direct charge semiconductor detector is mounted. With this detector, 210 nuclides can be monitored simultaneously with an average of 20 channels per nuclide. Every channel is a combination of two detector arrays with different signal amplifiers. In this way, it is possible for the detector to cover 6 orders of magnitude of working range in a single measurement; additional orders of magnitude can be covered when using extended measuring time. A schematic representation of the ion optical setup and the instrument is provided in Fig. 19.

Fig. 19 Schematic drawing of the *Spectro MS* (*Spectro*) (source: Spectro Analytical Instruments).

The range of applications for the new Spectro MS is diverse. The manufacturer sees the most important application areas in research and development laboratories with extremely high sample throughput and high demand. With its precision, sample throughput rate and permanent complete information on the entire mass spectrum with every measurement, Spectro Analytical Instruments expects to establish this instrument as the benchmark system for many new application areas. Especially when using laser ablation as a means of sample introduction, this full spectrum simultaneous monitoring is of great interest. Also for the emerging field of nano-particle analysis, this feature is extremely interesting. New applications can be developed with the option to simultaneously examine multiple isotope ratios even in mass ranges that lie far apart, together with the ability to transfer the precision of the isotope ratio analysis to the quantitative determination of element contents using a multiple isotope dilution approach (for more details see ref. 144).

6 Operational conditions

Most facets of using an ICP-MS instrument for trace element determination, such as calibration, quantification, use of internal standards and use of matrix-matched solutions, are identical for most types of ICP-MS instruments. Nevertheless there are a few significant differences in operation compared with quadrupole-based instrumentation, which will be discussed here in more detail.

6.1 Operation of single collector instruments

6.1.1 Scan modes. As has already been mentioned (see section 4.1), two different scan modes are routinely applied in sector field devices. Either the magnetic field strength is varied in a so-called B-scan or, alternatively, the acceleration voltage is varied in a so-called *E*-scan. Due to self-induction in the magnet coils, the scan speed in the B-scan is limited, but owing to special electronics, the cycling from ^{7}Li to ^{238}U and back to ^{7}Li can be achieved with a magnet settling time of 90 ms only. *E*-scan is an even faster scan mode with a settling time of one millisecond only. In this scan mode, the electric sector (E) and the accelerating voltages (U) are scanned simultaneously, to maintain the ratio E^2/U at a constant value, equal to the value providing transfer of the main beam of ions through the electric sector. The magnetic sector field is then set at a fixed value, such that main-beam ions of a predetermined m/z are transmitted by the magnetic field. At a first glance, the *E*-scan may be advantageous, but due to a loss of sensitivity at larger mass ranges (accelerating voltage decreases much), it is never applied to cover the whole mass range and is therefore restricted to a partial mass range of about 30–40% of the magnet mass only. In the low resolution mode, the preferred scanning mode of the instrument is peak hopping, as is the case for quadrupole mass analysers, too. With the *Element 2*/*XR*, this is usually done by setting the magnet to a particular mass and scanning a small range at the corresponding peak top *via* an *E*- scan, then jumping to the next mass

of interest by changing the accelerating voltage, followed by scanning the next peak, again using an *E*-scan. This procedure is applied until the maximum *E*-scan range for the particular magnet mass is reached. Subsequently, the magnet setting is changed to address the next mass range of interest. In the high mass resolution mode, the peak shape usually changes from a flat-topped into a triangular shape.[145] As a consequence, it is no longer the peak top only that is scanned, but the entire peak (or a fraction thereof) of the nuclide of interest. Otherwise, the same scan strategy as for low resolution mode is applied.

There are additional scan modes like the SynchroScan at the *Element 2*/*XR*, wherein a combination of *B*- and *E*-scanning is used. In this scan mode, the magnet field is increased continuously and the acceleration voltage is changed in a saw tooth manner. Therefore, the acquisition is carried out always at the centre of a peak with nearly optimum acceleration voltage before jumping to the next peak and thus, the duty cycle is high since there is no loss due to magnet settling times.

With the *AttoM*, ion optics are used to alter ion trajectories within the magnet in combination with fast magnetic scanning to increase the integration time on selected isotopes during elemental analysis along the whole mass range. For the fast magnetic scanning, the Hall probe control of the magnet is switched off. A high voltage is switched onto the magnet for 100 ms with the result that the magnet field increases linearly, thus permitting the whole mass range from 6 to 250 u to be scanned. During this period, the ion counter captures data at 10 μs intervals. After 100 ms, the high voltage is turned off and the magnet de-energises. In this way, the mass range from 250 to 6 u is rescanned. During both (up and down) periods, two datasets are acquired for each full magnet cycle. The next cycle starts after a 20 ms wait time.

6.1.2 Mass resolution. Commercially available instruments show a maximum mass resolution of typically up to ~10 000, although a mass resolution of up to 43 000 has been reported for a sector field ICP-MS device.[146] The resolution of the magnetic sector is constant over the whole mass range, whereas in quadrupole-based instruments, the mass analyzer is operated such that the peak width is constant over the mass range.

From the eqn (3.3.1), the consequences can be derived easily:

$$R = \frac{m}{\Delta m} \qquad (3.3.1)$$

With the constant resolution of magnetic sector instruments, the peak width is smaller at lower masses compared to higher masses, whereas the resolution of a quadrupole instrument varies with mass, *i.e.* it is lower at lower masses.

The final mass resolution for a given analyser geometry is determined by the widths of the source (entrance) and exit slit and the analyser geometry, as explained earlier. Because of the mechanical definition of the ion beam using slits, the peak shapes formed by magnetic sector instruments are ideally either flat-topped or triangular. In practice, the latter peaks are more Gaussian shaped.

The type of peak shape is defined by the ratio of the widths of the entrance and the exit slits. If the source (entrance) slit is considerably smaller than the exit slit, flat-top peaks are obtained, whereas when both slit widths are of similar width (depending on the design of the analyser), triangular peak shapes are obtained in theory.

The advantage of flat-topped peaks is that the measured ion beam intensity is constant over the mass range corresponding to the flat peak top, so that small deviations in the mass calibration are not affecting the result and thus, an improved isotope ratio precision can be achieved compared to quadrupole instruments. These peak shapes are also very well suited to operate the instrument in a peak hopping mode. Usually, this peak shape is obtained in low resolution mode ($R \sim 300$), but is not limited to it. At the highest resolution setting however, triangular peak shapes are typically observed.

It should be pointed out that increasing the resolution is always inherently connected with a loss of sensitivity, because the source slit (entrance slit) transmits only a fraction of the ion beam. This fractional transmission is defined by the ratio of the source slit size in the dispersive plane, to the size of the incident ion beam directed onto it and thus, decreases with decreasing slit width. Operational principles for MC-ICP-SFMS devices are given in 6.2.

6.1.3 Mass calibration. Due to the fact that sector field devices are always operated at fixed resolution, the peak width is changing over the mass range, with smaller width at lower masses. Compared to the peak width of typically ~0.7 u for quadrupole-based instruments, the peak width with a double-focusing magnetic sector instrument for, *e.g.*, ^{7}Li at a mass resolution of 10 000 is only 0.0007 u. Consequently, the requirements concerning accuracy and stability of the mass calibration are significantly higher for sector field instruments than for quadrupole-based instruments.

Therefore, the magnetic field is usually controlled by a feedback loop with the determination of the magnetic field at a representative location at the magnet, accomplished *via* either a Hall probe or another type of magnetic sensor. The generation of the magnetic field is accomplished by applying a particular current to the coils of the magnet. The operator just enters the isotope of interest into the steering software and, *via* the mass calibration, this input is converted by means of a DAC (digital-to-analogue converter) into a specific value that is provided to the control electronics, which then applies the required current to the magnetic coils. To perform a mass calibration, a solution containing defined elements is introduced into the ICP-MS and subsequently, a scan at a mass range around the expected mass of the nuclides or interferences is performed. The DAC value corresponding to the centroid of the acquired peak together with the accurate mass of the isotope is then entered in the mass calibration table. Depending on the sensor used, the electronics applied and the fact (see eqn (4.1.6).) that the mass is proportional to the square of the magnetic field, the relationship between mass and the digital control (DAC = digital analogue converter) may not be linear. Due to the fact that the peak width at low masses is smaller, it is preferred to have a steeper calibration curve, *i.e.* the change in mass per DAC step is smaller. Fit functions are used to calibrate the entire mass range on the basis of experimentally calibrated masses, distributed over the entire mass range of the mass spectrometer.

In order to reliably operate the instrument at higher resolution while scanning only a small mass range around the nuclide of

interest, the mass calibration has to be very stable. This is usually achieved by very stable electronics and by using the lock mass technique. Here, an ion signal that is always present in the spectrum, *e.g.*, that from $^{40}Ar^{40}Ar^{+}$, is used to dynamically and automatically adjust the mass calibration between analyses. With the *Element 2*/*XR*, *e.g.*, the mass stability is better than 25 ppm without performing mass calibration for months. This allows the use of small mass scan ranges of 1.2 peak widths in the highest resolution mode and thus allows, short overall analysis times.

6.2 Operation of multi-collector instruments

Operation principles as described in the following section are mainly based on the currently commercially available instruments, the *Neptune* and the *Nu Plasma II*.

6.2.1 Static mode. In contrast to single collector instruments, where scanning is required to direct the ions of interest sequentially into the detector, multi-collector devices are generally operated in static mode: the magnetic field is kept constant and the isotopes of interest are simultaneously measured using an array of Faraday collectors. As a consequence, isotope ratio measurements can be accomplished with very high precision.

In MC-ICP-SFMS devices, the electric sector has to be placed before the magnet and thus both the *Neptune Plus* as well as the *Nu Plasma II* are using Nier–Johnson geometry. The ESA compensates for the energy dispersion and focusing of the magnetic field. The magnet of a MC-ICP-MS device is set to a constant field in order to direct the central mass into the central detector. The other ions have to be directed into the adjacent detectors, whereby the separation between adjacent detectors depends on the mass dispersion of the magnet. The mass dispersion is up to 17% for the *Neptune Plus* and about 15% for the *Nu Plasma II*. The steering of the ions into the detectors is accomplished by two different methods:

The *Neptune Plus* uses movable cups which are moved mechanically to the position of the ion beam by means of motorized detector carriers, which can be equipped either with Faraday cups, channeltron ion counters or discrete dynode multipliers. An additional dynamic zoom lens system is positioned in-between the magnet and the detectors. It supports analysis at high mass resolution and enhances multi-dynamic measurements by applying variable zooming for different measurement sequences.

The *Nu Plasma II* has a variable dispersion zoom lens system behind the magnetic sector. As the location of the ion beam is adjusted by changing the dispersion of the zoom lens only, no moveable cups are required. As a consequence, the instrument can be operated in a dynamic mode. By changing the magnetic field along with the lens settings of the zoom lens system, a different set of isotopes can be analyzed. As no cup movement is involved, the switching delay between subsequent sequences is only some seconds.

6.2.2 Isotope ratio measurements. Isotope ratio analysis by MC-ICP-SFMS is accomplished by measuring simultaneously the intensity of the ion beams of interest for a preselected time (usually a couple of seconds). The measured signals are integrated and ratios are calculated. This is repeated several times, leading to a subset of ratios, from which the mean and standard deviation can be calculated. In contrast, single collector instruments have to measure the signal intensities for the isotopes of interest sequentially as fast as possible in order to establish a so called 'pseudo simultaneous measurement' (see Fig. 20). The latter means a fast switching between the isotopes of interest (during the time the signal intensity for isotope M1 is measured, no data are accumulated for M2 and *vice versa*) and data accumulation for a specified period of time. This subset of data is again integrated and an isotope ratio is calculated. This is repeated for n times. The final ratio is calculated as average of the single ratios from which the standard deviation is calculated as well. It is important that, *e.g.*, blank corrections and interference corrections apply to signal intensities and are accomplished prior to calculating the ratios whereas, *e.g.*, mass bias correction is conducted on the final ratio. This also has a specific impact on the proper calculation of total combined uncertainties. More details on isotope ratio determination are given in a specific tutorial.[147]

6.2.3 Mass resolution. In order to obtain flat top peaks, MC-ICP-SFMS instruments are usually operated at a mass resolution of about $m/\Delta m = 300$ to 400 (10% valley definition).

Nonetheless, a large number of isotopes show spectral interferences – even after target element isolation – which as a consequence influence isotope ratio measurements. Therefore, a number of interfered isotopes were not accessible for accurate isotope ratio measurements before the implementation of high resolution capabilities into MC-ICP-SFMS devices. Both, the *Neptune Plus* as well as the *Nu Plasma II*, allow operation in a pseudo high mass resolution mode by use of pre-selectable slits. The *Nu Plasma 1700* is a large geometry MC-ICP-SFMS which shows a mass dispersion enabling full mass resolution of up to 5000 in standard operating conditions.

The use of a defining slit results in a smaller beam geometry and as a result, analyte and interfering ions can be separated

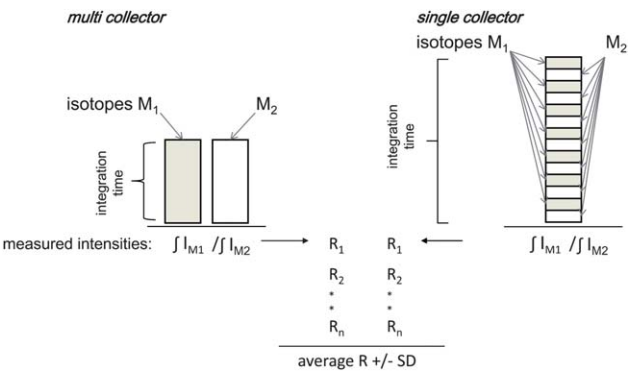

Fig. 20 Schematic representation of isotope ratio measurements using multi-collector and single collector ICP-MS: while with multi-collector ICP-MS, the signal intensities of the isotopes M1 and M2 are measured simultaneously throughout the entire measurement, the total integration time has to be divided between the two isotopes in the case of single-collector ICP-MS. In order to mimic simultaneous monitoring to the largest possible extent when using a single collector, M1 and M2 are monitored alternately at a sufficiently high peak hopping speed.

from one another. By using an imaging slit of the same dimension as the defining slit in front of the detector, a fully resolved mass spectrum can be obtained (Fig. 21). Nonetheless, the use of an imaging slit in MC-ICP-SFMS is not always useful. In case of moveable detectors (*Neptune*), each detector has to be equipped with a high resolution imaging slit. This would result in a tedious change of detectors in case of switching from low to high resolution. In case of fixed detectors (*Nu Plasma II*), a grid of slits can be moved mechanically in front of the detector entrances, resulting in the gradual reduction of the entrance width and thus defining an imaging slit width. Nonetheless, high mass resolution results in the loss of flat top peak shapes and thus deteriorates the precision of isotope ratio measurements significantly. As a consequence, MC-ICP-SFMS instruments are more generally operated in edge resolution mode (sometimes referred to by Nu Instruments as "pseudo high resolution mode") when high resolution capabilities are required in order to separate the analyte ion of interest from an interfering ion.[148] In edge resolution, a defining slit is used to reduce the ion beam width. As a consequence, interfering ions can be separated from the ions of interest. The beam is subsequently directed towards the slit in front of the detector in such way, that the interfering beam is simply clipped on one side of the collector slit while the analyte beam is collected in the detector (see Fig. 22). Fig. 22 shows that the width of the incoming ion beam (analyte + interference) is defined by the entrance (defining) slit. The magnet leads to the separation of the analyte and interference. In magnet position 1, the analyte can be measured non-interfered since the interference is clipped on the left side of the detector. When scanning the mass spectrum up to a mass-to-charge ratio of ~80, most interferences are occurring on the high mass side: Therefore, the first shoulder corresponds to the analyte of interest, the highest platform is the result of the analyte signal plus that of the interference and the second shoulder corresponds to the interference only. The magnet is set such that static analysis is accomplished at the first shoulder.

This approach of edge resolution, which was introduced by Thermo Fisher Scientific on the *Neptune*, and does not fully resolve interferences, achieves high precision in isotope ratio measurements by ensuring that adequate interference separation is achieved, while retaining flat top peak profiles (flat shoulders). This approach was adopted on the *Nu Plasma II* instrument and is shown for S isotope ratio measurements. The $^{34}S/^{32}S$ isotope ratio measurements using a solution containing 2 μg g^{-1} S leads to a average precision (repeatability) of better than 0.007% when applying pseudo high mass resolution whereas the precision deteriorates to average 0.013% when applying full high resolution mode.

It is evident that small mass drifts have no significant effect on the final ratio when low mass resolution is applied as long as flat top peaks are maintained. This is different in high resolution mode, as small drifts can already lead to a significant change of the isotope ratio precision. Therefore, control of temperature, amongst some other parameters, is of crucial importance.

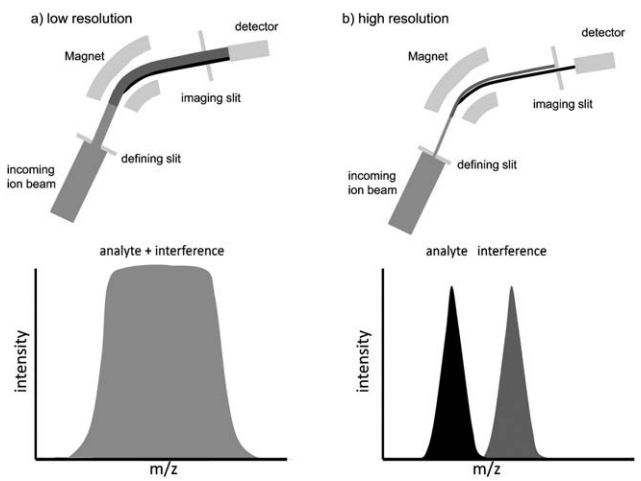

Fig. 21 Schematic of the measurement at (a) low and (b) high resolution using ICP-SFMS.

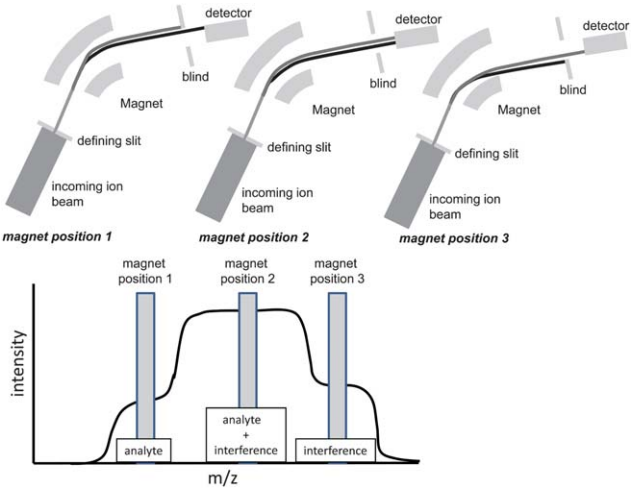

Fig. 22 Schematic representation of measurement at 'pseudo high resolution' using multi-collector ICP-MS. Lower figure: mass spectral peak obtained upon scanning the mass range of interest. The signals of analyte and interfering ion are not completely resolved, but three peak sections can be recognized - from left to right: contribution of analyte ion only, contribution from both analyte and interfering ion and contribution from interfering ion only. Final data acquisition is carried out under the conditions represented by the upper left figure: only analyte ions are admitted to enter the detector. For completeness, also the situation wherein both ions contribute to the signal and wherein only the interfering ion contributes to the signal have been shown in the upper part as the middle and right figure, respectively.

6.3 Mass discrimination

The large instrumental mass discrimination which is a result of the preferential extraction and transmission of heavier isotopes is a significant property of ICP-MS (a more detailed discussion is given in ref. 149). As a result, an isotope ratio measured with ICP-MS may show significant bias with respect to the corresponding true value. This phenomenon is referred to as mass discrimination and it ranges from 0,5–1,5% per mass unit for heavier masses and up to 15% for light masses. As a consequence, proper correction for mass discrimination is essential. Adequate correction for mass discrimination is still a challenge, especially

as it is affected by both the matrix, the analyte concentration and operational conditions of the instrument. Even after isolation of the target element – a common approach when pneumatic nebulization is used for sample introduction into MC-ICP-SFMS – proper correction for mass discrimination is not self-evident. Various approaches have been developed and there is still considerable debate among the specialists as to which approach provides the best results.

In single collector devices, scanning is accomplished by changing the acceleration voltage. As different isotopes are then analyzed at different acceleration voltages, additional mass bias effects can be observed which are reverse to the previously described. This is a consequence of the 'Liouville theorem'.[150] It can be seen as the homogeneous form of the Boltzmann transport equation and is explained in any good book on classical mechanics. Therefore, it is evident that the mass bias observed in single collector instruments strongly depends on the instrumental setting. As a consequence, negative or positive bias can be observed. When peak shifts are corrected for by changing scan parameters (*e.g.*, acceleration voltage), changes in mass bias may effect isotope ratio measurements. To keep the acceleration voltage constant, the *AttoM*, *e.g.*, corrects for peak shifts by beam deflection at constant acceleration voltage and ESA settings.

6.3.1 External mass bias correction. In this approach, a solution containing an isotopic standard of the target element (with a known isotopic composition) is measured before or after the sample. Bracketing – whereby the measurement of each sample solution is preceded and followed by a measurement of the isotopic standard – provides the optimum results as it covers any instrumental drift. A correction factor is calculated on the basis of the observed bias between the measured value and the true value of the isotope ratio of interest.

$$k = R_{\text{true}}/R_{\text{measured}}$$

The matrix exerts a quite pronounced influence on the extent of mass discrimination (depending on the mass of the isotopes) and therefore, it is preferable if the target element is isolated from the matrix. The removal of possible interfering elements is an additional advantage. (*e.g.*, separation of ^{87}Rb from ^{87}Sr).[151–153] It is even advantageous if the concentration of the target element in the samples matches the standards within ± 30%.[154] The standards are preferably certified reference materials with certified isotopic composition, which are available for a range of commonly investigated elements. Alternatively, 'natural' standards are used and their isotopic composition taken from the IUPAC tables.[155] It is clear that the latter approach is only sufficient for, *e.g.*, isotope dilution purposes, since the measurement of natural variations of isotopic composition could be affected by a systematic bias or at least an increased uncertainty. In case of isotope dilution mass spectrometry, it is preferable if the isotopic composition of the standard matches the isotopic composition of the blend, which is not always achievable.[156]

As an example for external correction, ^{87}Sr/^{86}Sr isotope ratios can be corrected for externally by using the NIST SRM 987 $SrCO_3$ with a certified isotopic composition of ^{87}Sr/^{86}Sr = 0.71034 ± 0.00026 (National Institute of Standards and Technology, Gaithersburg, USA).[151] A value of 0.710245 has been used by the geological community.[157]

6.3.2 Internal mass bias correction. Internal correction is applied if an isotopic pair is available in the sample with invariant and known isotope ratio. This can be either an invariant isotope pair of the target element or of a different element (mostly preferable of similar mass and chemical properties). This element can be part of the sample already or can be added into the sample. In the latter case, preferably a certified reference standard has to be used. Otherwise, the isotopic composition of elements with little naturally occurring fractionation can be derived from the IUPAC tables, even though a certain possible systematic bias might be taken into account.[155] Several approaches can be used for correcting the investigated isotope pair, depending on whether it is assumed that mass discrimination varies according to a linear, a power-law or an exponential function by taking into account the difference in mass between the two isotopes Δm:[158,159]

$$K = \frac{R_{\text{true}}}{R_{\text{obs}}} = (1 + \varepsilon_{\text{linear}}\Delta m)$$
$$K = \frac{R_{\text{true}}}{R_{\text{obs}}} = \left(1 + \varepsilon_{\text{power}}\right)^{\Delta m} \qquad (6.2.1\text{a–c})$$
$$K = \frac{R_{\text{true}}}{R_{\text{obs}}} = \mathrm{e}^{\left(\varepsilon_{\text{exponential}}\Delta m\right)}$$

In Russell's equation[150,151] on the other hand, the mass of the isotopes rather than the mass difference between them is considered as the factor determining the extent of mass discrimination:

$$K = \frac{R_{\text{true}}}{R_{\text{obs}}} = \left(\frac{m_1}{m_2}\right)^{\beta} \qquad (6.2.2)$$

A further refinement in this approach consists of establishing a linear relationship between the mass discrimination values per mass unit for the target element and the internal standard, respectively, on the basis of standard solutions. For the actual samples, the experimentally measured β or ε value for the internal standard can then be converted into that for the target element, as exemplified for Pb and Tl in Fig. 23 (figure provided by the RSC from ref. 13 with permission from the author ref. 160).

Coming back to the example for mass bias correction for Sr isotope ratios, the following procedure using the 'exponential law of mass bias correction' has been widely accepted and adapted for routine use in the geochemical community: Therein, the fractionation factor of Sr is calculated by the use of the internal ^{88}Sr/^{86}Sr ratio in a first step. (The strategy is based on the circumstance that the ^{88}Sr/^{86}Sr ratio is assumed to be stable in nature[161] even though recent investigations show that natural variation can occur.[162] This has of course an impact on the correction strategy.) In the following, the correction of ^{87}Sr for its isobaric interference ^{87}Rb is accomplished using the ^{85}Rb/^{87}Rb ratio.[163–165] (This is made necessary as residual Rb can occur and experimental approaches for Sr matrix separation are, *e.g.*, not applicable so far in LA-ICP-MS.) Besides, the mathematical Rb correction of ^{87}Sr/^{86}Sr is questionable as it has been shown that an increase of the Rb concentration in the sample leads to

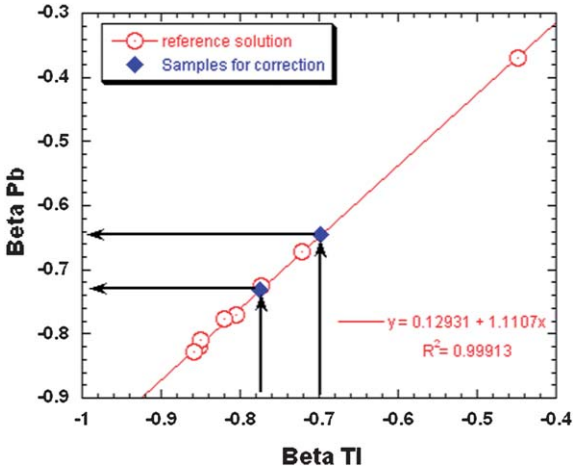

Fig. 23 Relationship (red line) between the mass discrimination factors for Tl (internal standard) and Pb (target element) as established using measurements on standard solutions (red circles). This experimentally determined relationship can then be used to convert the mass discrimination factor for Tl into that for Pb for the samples, as demonstrated for two data points displayed as blue diamonds.

a systematic shift of $^{87}Sr/^{86}Sr$ when assuming similar discrimination of Sr and Rb in the ICP-MS.[153,166,167] As an alternative, Zr is added and Zr isotopes are used to correct for the mass bias on $^{87}Sr/^{86}Sr$.[162]

As other examples, *e.g.*, Tl is used in Pb[168] or Hg[169,170] analysis or Zr in Mo isotopic analysis.[171] The bias between the measured $^{203}Tl/^{205}Tl$ or $^{90}Zr/^{91}Zr$ isotope ratio and the corresponding true value is used to determine the mass discrimination per mass unit ε, which is subsequently used to correct the Pb, Hg or Mo isotope ratio data for mass discrimination.

6.3.4 Other approaches. There is an ongoing debate as to which correction method provides the most accurate description of mass discrimination effects. This is an issue of increasing importance as a result of the continuously improving isotope ratio precision attainable. Other approaches – such as the generalized power law[172] or a double spike approach[173] – have been reported to provide even more accurate results. For more information on these approaches, the reader is referred to the specialized literature.

6.4 Detector issues

6.4.1 Detector dead time. Detector dead time is an effect which is observed for electron multipliers operated in pulse counting mode. This effect does not exist neither for electron multipliers operated in analogue mode nor for Faraday cups. When an electron multiplier is used in a pulse counting mode for measuring the signal intensity, a certain dead time of the detector and its associated electronics exists, in which subsequent ion pulses cannot be determined. The detection and electronic handling of every pulse typically takes 5–100 ns (depending on the type of multiplier and electronics used) and another ion arriving at the detector within a shorter time frame after a first one will not be detected. Self-evidently, this leads to signal losses that become more pronounced as the rate of ions arriving at the detector increases. As a result, measurement data for isotope ratios differing from unity will show a bias with respect to the corresponding true value. Also the linearity of a calibration curve at higher concentrations (higher count rates) will considerably be influenced. Detectors are categorized in paralyzable and non-paralyzable ones. A non-paralytic detector is seen as a detector where the arrival of a second ion within the time required for handling the first one (deadtime) does not lead to an extension of the time during which the detector is 'dead' or in other words not capable of detecting another incoming ion. Usual detectors are between paralyzable and non-paralyzable types. For the latter type, the actual count rate can be calculated from the observed count rate, provided that the dead time τ is known.[174]

$$\frac{1}{\text{observed count rate}} = \frac{1}{\text{actual count rate}} + \tau \text{ (in s)} \quad (6.2.3)$$

As a consequence, the dead time of the detector system has to be determined experimentally. Although there are various approaches for experimental determination of the dead time,[175] they are all based on the fact that appropriate correction of the measured signal intensities for dead time losses should result in a sensitivity (signal intensity/concentration unit) independent of the signal intensity and hence, independent of analyte concentration.

The software of all ICP-SFMS instruments provides the possibility of automatic correction for detector dead time. Some instruments however, use a predefined value that is not accessible by the user. Although this may be sufficient to some extent for element determination, it is not an acceptable situation for accurate isotope ratio determination. Some instruments provide an automated means for the determination of the detector dead time, *e.g.*, based on the measurement of a single signal, the intensity of which is changed by adapting the voltage applied to the extraction lens and/or comparison of pulse-counting and analogue intensities.[176] The most reliable methods for dead time determination however rely on the measurement of a given isotope ratio in standard solutions showing a sufficiently wide

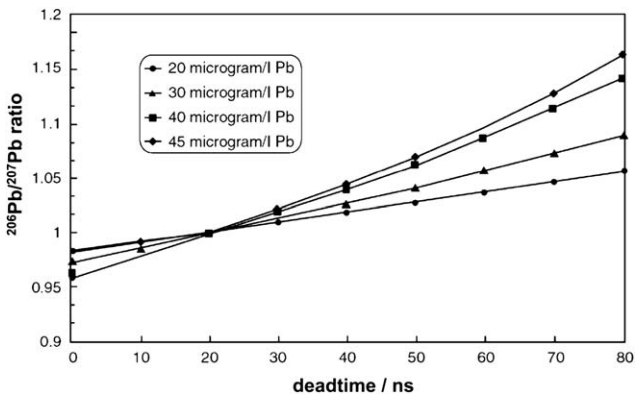

Fig. 24 Russ' method for determination of detector dead time (electron multiplier in pulse counting mode). Experimental ($^{206}Pb/^{207}Pb$) ratio, corrected for detector dead time using a range of assumed values (*x*-axis), divided by the corresponding true value for standard solutions with different Pb contents. The lines thus observed (ideally) intersect in one point, the x-value of which corresponds to the actual dead time.

range of analyte concentrations. In Russ' method,[177] a series of standard solutions of a given element, spanning a sufficiently wide concentration range, are measured. The value that the instrument's software is using for automatic correction for detector dead time has to be set to zero for these measurements. Next, for each standard solution, the signal intensities of the two isotopes selected are corrected for dead time losses assuming a number of detector dead time values in an appropriate range and the isotope ratios thus obtained are plotted as a function of the value applied for correction for each of the standard solutions measured (Fig. 24 from ref. 177). For each concentration level, the values thus obtained lay on a line and the lines for the various concentration levels (should) intersect in one point (x,y), The x-value provides the analyst with the detector dead time, the bias between the y-value and the corresponding 'true' value on the other hand, reflects the extent of mass discrimination.

6.4.2 Sag. When using an electron multiplier in the pulse counting mode, the amplitude of every individual pulse is compared with a threshold value by a 'discriminator'. In this way, it is possible to avoid 'false' signals (*e.g.*, resulting from ionization of residual gas molecules in the detector as a result of the electron multiplication effect) from contributing to the measured intensity. However, at very high count rates, the gain of an electron multiplier is reduced to such an extent that a substantial fraction of the incoming ions give rise to an output pulse that is actually below the threshold. As a result, much more pronounced signal losses than expected on the basis of the detector dead time occur and cannot be adequately corrected for. This phenomenon is referred to as sag and should be avoided in isotope analysis.[178–180]

6.5 Detector calibration in multi-collector arrays

As has been said already, neither for electron multipliers operated in analogue mode, nor for Faraday cups, detector dead time effects occur. However, if Faraday cups are used in a multi-collector array whereby each cup has its own amplifier, these individual detectors have to be cross-calibrated in order to provide the same sensitivity.

For traditional systems, the need for a precise cross-calibration of the current amplifiers defines a precision barrier in static multi-collection. Even with perfect Faraday cups giving uniform response, results of static measurements are biased by the accuracy and reproducibility of the gain calibration. In the traditional method of cross calibration, a high precision, constant current source is sequentially connected to all amplifiers. However, with this method, amplifiers cannot be calibrated to better than ~5 ppm per channel. The goal of the new multi-collector development was to break through the 5 ppm precision barrier. The *Neptune* uses a patented measurement procedure, which completely eliminates gain calibration biases: the Virtual Amplifier concept.[181] In all previous multi-collector systems, the relation (connection) between individual Faraday cups and amplifiers was fixed. In the Virtual Amplifier concept, all Faraday cups involved in a certain measurement are sequentially connected to all amplifiers. As a result, all signals have been measured with the same set of amplifiers and for the calculation of the isotope ratios, all calibration biases of the amplifiers are cancelled.

Cross-calibration of Faraday cups and electron multipliers is usually accomplished by direct measurement of isotope pairs of a certified reference material and by assessing external correction factors.

7 Summary

In this review, the basic concepts of sector field instruments have been introduced with the main focus onto fundamentals, instrumentation and instrument operation. A proper overview of the capabilities of the commercially available instrumentation has now been given. In part II, selected applications will be presented to further discuss the peculiarities, performance and analytical figures of merit of sector field devices in different areas of applications. Finally, future trends and developments will be pinpointed.

Acknowledgements

Fruitful discussions, corrections and contributions from Charles B. Douthitt are thankfully acknowledged.

References

1 L. Moens and N. Jakubowski, *Anal. Chem.*, 1998, **70**, 251–256.
2 N. Jakubowski, L. Moens and F. Vanhaecke, *Spectrochim. Acta, Part B*, 1998, **53**, 1739–1763.
3 N. Jakubowski, L. Moens and F. Vanhaecke, *Spectrochim. Acta, Part B*, 1998, **53**, 1739–1763.
4 N. Jakubowski, *J. Anal. At. Spectrom.*, 2008, **23**, 673–684.
5 G. M. Hieftje, *J. Anal. At. Spectrom.*, 2008, **23**, 661–672.
6 J. S. Becker, *Inorganic Mass Spectrometry – Principles and Applications*, 2007, John Wiley & Sons, Chichester.
7 S. M. Nelms (Ed.): *ICP Mass Spectrometry Handbook*, Blackwell Publishing, ISBN: 0-8493-2381-9.
8 F. Vanhaecke and G. Koellensperger, *Detection by ICP-MS: Handbook of Elemental Speciation, Techniques and Methodology*, ISBN 0-471-49214-0, Ed. by R. Cornelis, J. Caruso, H. Crews, and K. G. Heumann, Publ. John Wiley & Sons, 2003, 5.3, 281–312.
9 A. Montaser, *Inductively Coupled Plasma Mass Spectrometry*, Wiley-VCH, New York, 1998.
10 R. Thomas, *Practical Guide to ICP-MS, Series Practical Spectroscopy*, Marcel Dekker, New York, 2004, 33.
11 J. S. Becker, *Inorganic Mass Spectrometry – Principles and Applications*, 2007, John Wiley & Sons, Chichester.
12 A. N. Halliday, J. N. Christensen, D.-C. Lee, C. M. Hall, X. Luo, and M. Rehkaemper, Multi-Collector Inductively Coupled Plasma Mass Spectrometry. In: *Inorganic Mass Spectrometry – Fundamentals and Applications, Practical Spectroscopy Series Volume 23*; C. M. Barshick, D. C. Duckworth, D. H. Smith, ed.; M. Dekker: New York, USA, 2000; 291–329.
13 F. Vanhaecke, L. Balcaen and D. Malinovsky, *J. Anal. At. Spectrom.*, 2009, **24**, 863–886.
14 K. Robinson and R. Naylor, *Europ. Spectrosc. News*, 1986, **68**, 18–22.
15 N. Bradshaw, E. F. H. Hall and N. E. Sanderson, *J. Anal. At. Spectrom.*, 1989, **4**, 801–803.
16 M. Morita, H. Itoh, T. Uehiro and K. Otsuka, *Anal. Sci.*, 1989, **5**, 609–610.
17 U. Giessmann and U. Greb, A New Concept for Elemental Mass Spectrometry. Presented at the *2nd Regensburg Symposium on "Massenspektrometrische Verfahren der Elementspurenanalyse"*; 1993; paper DV1.
18 C. B. Douthitt, *J. Anal. At. Spectrom.*, 2008, **23**, 685–689.
19 J. J. Thomson and G. P. Thomson, *Conduction of Electricity through Gases*, Cambridge University Press, 1928, 1.
20 F. W. Aston, *Mass Spectra and Isotopes*, Longmans: New York, 1942.
21 A. J. Dempster, *Proc. Am. Phil. Soc.*, 1935, **75**, 755–767.

22 A. J. Dempster, *Rev. Sci. Instrum.*, 1936, **7**, 46–49.
23 A. O. Nier, *Rev. Sci. Instrum.*, 1940, **11**, 212–216.
24 E. G. Johnson and A. O. Nier, *Phys. Rev.*, 1953, **91**, 10–17.
25 F. W. Aston, *Mass Spectra and Isotopes*, Longmans, New York, 1942.
26 J. J. Thomson and G. P. Thomson, *Conduction of Electricity through Gases*, Vol. 1, Cambridge University Press, 1928.
27 A. J. Dempster, *Proc. Am. Phil. Soc.*, 1935, **75**, 755–767.
28 G. Ramendik, J. Verlinden, and R. Gijbels, Spark Source Mass Spectrometry, *Inorganic Mass Spectrometry*, ed. by F. Adams, R. Gijbels and R. Van Grieken, John Wiley & Sons, New York, 1988.
29 J. W. Coburn, *Rev. Sci. Instrum.*, 1970, **41**, 1219–1223.
30 J. W. Coburn, E. W. Eckstein and E. Kay, *J. Vac. Sci. Technol.*, 1975, **12**, 151–154.
31 W. W. Harrison and C. W. Magee, *Anal. Chem.*, 1974, **46**, 461–464.
32 B. N. Colby and C. A. Evans, *Anal. Chem.*, 1974, **46**, 1236–1242.
33 D. L. Donohue and W. W. Harrison, *Anal. Chem.*, 1979, **51**, 673–678.
34 R. K. Marcus, *J. Anal. At. Spectrom.*, 1994, **9**, 1029–1037.
35 M. R. Winchester and R. Payling, *Spectrochim. Acta, Part B*, 2004, **59**, 607–666.
36 K. Robinson and R. Naylor, *Europ. Spectrosc. News*, 1986, **68**, 18–22.
37 C. Venzago, L. Ohanessian-Pierrard, M. Kasik, U. Collisi and S. Baude, *J. Anal. At. Spectrom.*, 1998, **13**, 189–193.
38 J. S. Becker, A. I. Saprykin and H.-J. Dietze, *Int. J. Mass Spectrom. Ion Processes*, 1997, **164**, 81–91.
39 A. I. Saprykin, J. S. Becker and H.-J. Dietze, *Fresenius' J. Anal. Chem.*, 1996, **355**, 831–835.
40 J. S. Becker and H.-J. Dietze, *Int. J. Mass Spectrom.*, 2000, **197**, 1–35.
41 H. Grimm, *Spectrochim. Acta, Part B*, 1968, **23**, 443–454.
42 N. Jakubowski, D. Stüwer and W. Vieth, *Anal. Chem.*, 1987, **59**, 1825–1830.
43 N. Jakubowski and D. Stüwer, *J. Anal. At. Spectrom.*, 1992, **7**, 951–958.
44 N. Jakubowski, I. Feldmann and D. Stuewer, *J. Anal. At. Spectrom.*, 1997, **12**, 151–157.
45 N. Jakubowski, I. Feldmann and D. Stuewer, *Spectrochim. Acta, Part B*, 1995, **50**, 639–654.
46 R. S. Mason, P. D. Miller and I. P. Mortimer, *Phys. Rev. E*, 1997, **55**, 7462–7472.
47 R. S. Mason, D. R. Williams, I. P. Mortimer, D. J. Mitchell and K. Newman, *J. Anal. At. Spectrom.*, 2004, **19**, 1177–1185.
48 P. D. Miller, D. Thomas, R. S. Mason, and M. Liezers, *Recent Advances in Plasma Source Mass Spectrometry*, ed. G. Holland, BPC Wheatons, Ltd, Exeter, UK, 1995, 91–101.
49 K. Newman, R. S. Mason, D. R. Williams and I. P. Mortimer, *J. Anal. At. Spectrom.*, 2004, **19**, 1192–1198.
50 V. Hoffmann, *Poster presented at the European Winter Conference on Plasma Spectrochemistry*, 2001, P4–38, Hafjell, Norway.
51 A. Bogaerts, A. Okhrimovsky and R. Gijbels, *J. Anal. At. Spectrom.*, 2002, **17**, 1076–1082.
52 C. Beyer, I. Feldmann, D. Gilmour, V. Hoffmann and N. Jakubowski, *Spectrochim. Acta, Part B*, 2002, **57**, 1521–1533.
53 J. Pisonero, I. Feldmann, N. Bordel, A. Sanz-Medel and N. Jakubowski, *Anal. Bioanal. Chem.*, 2005, **382**, 1965–1974.
54 D. A. Solyom, T. W. Burgoyne and G. M. Hieftje, *J. Anal. At. Spectrom.*, 1999, **14**, 1101–1110.
55 S. Greenfield, I. J. Jones and C. T. Berry, *Analyst*, 1964, **89**, 713–720.
56 A. Gray, *Analyst*, 1975, **100**, 289–299.
57 V. A. Fassel, *Science*, 1978, **202**, 183–191.
58 R. S. Houk, *Thesis*, Iowa State University, Ames, Iowa, 1980, IS-T-898.
59 R. S. Houk, V. A. Fassel, G. D. Flesch, J. J. Svec, A. L. Gray and C. E. Taylor, *Anal. Chem.*, 1980, **52**, 2283–2289.
60 A. R. Date and A. L. Gray, *Analyst*, 1981, **106**, 1255–1267.
61 R. S. Houk and J. J. Thompson, *Biol. Mass Spectrom.*, 1983, **10**, 107–112.
62 W. Tittes, N. Jakubowski, D. Stuewer, G. Toelg and J. A. C. Broekaert, *J. Anal. At. Spectrom.*, 1994, **9**, 1015–1020.
63 I. Feldmann, W. Tittes, N. Jakubowski, D. Stuewer and U. Giessmann, *J. Anal. At. Spectrom.*, 1994, **9**, 1007–1014.
64 N. Jakubowski, W. Tittes, D. Pollmann, D. Stuewer and J. A. C. Broekaert, *J. Anal. At. Spectrom.*, 1996, **11**, 797–803.
65 U. Giessmann and U. Greb, *Fresenius' J. Anal. Chem.*, 1994, **350**, 186–193.
66 A. J. Walder and P. A. Freedman, *J. Anal. At. Spectrom.*, 1992, **7**, 571–575.
67 A. J. Walder, I. Platzner and P. A. Freedman, *J. Anal. At. Spectrom.*, 1993, **8**, 19–23.
68 N. S. Belshaw, P. A. Freedman, R. K. O'Nions, M. Frank and Y. Guo, *Int. J. Mass Spectrom.*, 1998, **181**, 51–58.
69 D. A. Solyom, T. W. Burgoyne and G. M. Hieftje, *J. Anal. At. Spectrom.*, 1999, **14**, 1101–1110.
70 J. H. Barnes IV, R. P. Sperline, M. B. Denton, C. J. Barinaga, D. W. Koppenaal, E. T. Young and G. M. Hieftje, *Anal. Chem.*, 2002, **74**, 5327–5332.
71 G. D. Schilling, F. J. Andrade, J. H. Barnes IV, R. P. Sperline, M. B. Denton, C. J. Barinaga, D. W. Koppenaal and G. M. Hieftje, *Anal. Chem.*, 2007, **79**, 7662–7668.
72 A. A. Rubinshtein, G. D. Schilling, S. J. Ray, R. P. Sperline, M. B. Denton, C. J. Barinaga, D. W. Koppenaal and G. M. Hieftje, *J. Anal. At. Spectrom.*, 2010, **25**, 735–738.
73 G. D. Schilling, S. J. Ray, A. A. Rubinshtein, J. A. Felton, R. P. Sperline, M. B. Denton, C. J. Barinaga, D. W. Koppenaal and G. M. Hieftje, *Anal. Chem.*, 2009, **81**, 5467–5473.
74 D. Ardelt, U. Heyen, *First results with a new multichannel ion detector. Talk W05 at the 2010 Winter Conference on Plasma Spectrochemistry*, January 4–9, 2010, Fort Myers, Florida.
75 http://www.spectro.com/pages/e/p060124_New_Era_in_ICP_Mass_Spectrometry.htm.
76 E. I. Evans and J. J. Griglio, *J. Anal. At. Spectrom.*, 1993, **8**, 1–18.
77 I. Feldmann, N. Jakubowski, D. Stuewer and C. Thomas, *J. Anal. At. Spectrom.*, 2000, **15**, 371–376.
78 N. F. Zahran, A. I. Helal, M. A. Amr, A. Abedl-Hafiez and H. T. Mohsen, *Int. J. Mass Spectrom.*, 2003, **226**, 271–278.
79 N. Nonose and M. Kubota, *J. Anal. At. Spectrom.*, 2001, **16**, 551–559.
80 D. B. Aeschliman, S. J. Bajic, D. P. Baldwin and R. S. Houk, *J. Anal. At. Spectrom.*, 2003, **18**, 1008–1014.
81 K. C. Sears, J. W. Ferguson, T. J. Dudley, R. S. Houk and M. S. Gordon, *J. Phys. Chem. A*, 2008, **112**, 2610–2617.
82 M. Resano, F. Vanhaecke and M. T. C. de Loos-Vollebregt, *J. Anal. At. Spectrom.*, 2008, **23**, 1450–1475.
83 J. Pisonero, B. Fernández and D. Günther, *J. Anal. At. Spectrom.*, 2009, **24**, 1145–1160.
84 P. Wu, L. He, C. Zheng, X. Hou and R. E. Sturgeon, *J. Anal. At. Spectrom.*, 2010, **25**, 1217–1246.
85 S. Swoboda, M. Brunner, S. Boulyga, P. Galler, M. Horacek, G. Stingeder and T. Prohaska, *Anal. Bioanal. Chem.*, 2008, **390**, 487–494.
86 C. Latkoczy, T. Prohaska, M. Watkins, G. Stingeder and M. Teschler Nicola, *J. Anal. At. Spectrom.*, 2001, **16**, 806–811.
87 P. Galler, A. Limbeck, M. Uveges and T. Prohaska, *J. Anal. At. Spectrom.*, 2008, **23**, 1388–1491.
88 S. D. Tanner, V. I. Baranov and D. R. Bandura, *Spectrochim. Acta, Part B*, 2002, **57**, 1361–1452.
89 D. J. Douglas, *Can. J. Spectrosc.*, 1989, **34**, 38–49.
90 J. T. Rowan and R. S. Houk, *Appl. Spectrosc.*, 1989, **43**, 976–980.
91 G. C. Eiden, C. J. Barinaga and D. W. Koppenaal, *Rapid Commun. Mass Spectrom.*, 1997, **11**, 37–42.
92 P. Turner, T. Merren, J. Speakman, and C. Haines ed. by G. Holland, S. D. Tanner, Special Publication of the Royal Chemical Society, Cambridge, 1997, 202, 28–34.
93 I. Feldmann, N. Jakubowski and D. Stuewer, *Fresenius J. Anal. Chem.*, 1999, **365**, 415–421.
94 L. J. Moens, F. F. Vanhaecke, D. R. Bandura, V. I. Baranov and S. D. Tanner, *J. Anal. At. Spectrom.*, 2001, **16**, 991–994.
95 Z. Du, D. J. Douglas and N. Konenkov, *J. Anal. At. Spectrom.*, 1999, **14**, 1111–1119.
96 M. W. Soyk, Q. Zhao, R. S. Houk and E. R. Badman, *J. Am. Soc. Mass Spectrom.*, 2008, **19**, 1821–1831.
97 G. C. Eiden, C. J. Barinaga and D. W. Koppenaal, *J. Am. Soc. Mass Spectrom.*, 1996, **7**, 1161–1171.
98 P. P. Mahoney, S. J. Ray and G. M. Hieftje, *Appl. Spectrosc.*, 1997, **51**, 16 A–28 A.

99 K. E. Milgram, F. M. White, K. L. Goodner, C. H. Watson, D. W. Koppenaal, C. J. Barinaga, B. H. Smith, J. D. Winefordner, A. G. Marshall, R. S. Houk and J. R. Eyler, *Anal. Chem.*, 1997, **69**, 3714–3721.
100 C. H. Watson, J. Wronka, F. H. Laukien, C. M. Barshick and J. R. Eyler, *Spectrochim. Acta, Part B*, 1993, **48**, 1445–1448.
101 C. H. Watson, C. M. Barshick, J. Wronka, F. H. Laukien and J. R. Eyler, *Anal. Chem.*, 1996, **68**, 573–575.
102 A. Makarov, *Anal. Chem.*, 2000, **72**, 1156–1163.
103 K. J. R. Rosman and P. D. P. Taylor, *Pure Appl. Chem.*, 1998, **70**, 217–236.
104 W. F. Libby, *Phys. Rev.*, 1946, **69**, 671–672.
105 E. C. Anderson, W. F. Libby, S. Weinhouse, A. F. Reid, A. D. Kirshenbaum and A. V. Grosse, *Phys. Rev.*, 1947, **72**, 931–936.
106 B. Wohlfarth, *Quat. Sci. Rev.*, 1996, **15**, 267–284.
107 L. T. Silver and S. Deutsch, *J. Geol.*, 1963, **71**, 721–758.
108 R. R. Parrish, *Can. J. Earth Sci.*, 1990, **27**, 1431–1450.
109 L. P. Black, S. L. Kamo, C. M. Allen, J. N. Aleinikoff, D. W. Davis, R. J. Korsch and C. Foudoulis, *Chem. Geol.*, 2003, **200**, 155–170.
110 S. Swoboda, M. Brunner, S. Boulyga, P. Galler, M. Horacek, G. Stingeder and T. Prohaska, *Anal. Bioanal. Chem.*, 2008, **390**, 487–494.
111 T. Prohaska, W. Wenzel and G. Stingeder, *Int. J. Mass Spectrom.*, 2005, **242**, 243–250.
112 S. F. Boulyga and Thomas Prohaska, *Anal. Bioanal. Chem.*, 2008, **390**, 531–539.
113 G. Schultheis, T. Prohaska, M. Schreiner and G. Stingeder, *J. Anal. At. Spectrom.*, 2004, **19**, 838–843.
114 H. Craig, *Science*, 1961, **133**, 1702–1703.
115 H. Forstel and H. Hutzen, *Nature*, 1983, **304**, 614–616.
116 F. Wombacher, M. Rehkaemper, K. Mezger and C. Munker, *Geochim. Cosmochim. Acta*, 2003, **67**, 4639–4654.
117 F. Wombacher, M. Rehkaemper and K. Mezger, *Geochim. Cosmochim. Acta*, 2004, **68**, 2349–2357.
118 N. L. Allinger, M. P. Cava, D. C. de Jongh, C. R. Johnson, N. A. Lebel, and C. L. Stevens *Organische Chemie*, 1980, Walter de Gruyter Verlag, Berlin, 472–474.
119 M. R. Palmer, D. London, G. B. Morgan and H. A. Babb, *Chem. Geol.*, 1992, **101**, 123–129.
120 M. R. Palmer, A. J. Spivack and J. M. Edmond, *Geochim. Cosmochim. Acta*, 1987, **51**, 2319–2323.
121 G. Faure and T. M. Mensing, *Isotopes Principles and applications*, 3rd edition, John Wiley and sons, 2005.
122 D. R. Lide, (ed) *CRC Handbook of Chemistry and Physics*, CRC Press LLC, Boca Raton, 2001.
123 S. Stürup, H. Hansen and B. Gammelgaard, *Anal. Bioanal. Chem.*, 2008, **390**, 541–554.
124 C. Eis, M. Watkins, T. Prohaska and B. Nidetzky, *Biochem. J.*, 2001, **356**, 757–767.
125 T. Bohn, T. Walczyk, L. Davidsson, W. Pritzkow, P. Klingbeil, J. Vogl and R. F. Hurrell, *Br. J. Nutr.*, 2004, **91**, 113–120.
126 T. Bohn, L. Davidsson, T. Walczyk and R. F. Hurrell, *Br. J. Nutr.*, 2004, **91**, 601–606.
127 J. Vogl, *J. Anal. At. Spectrom.*, 2007, **22**, 475–492.
128 J. Vogl and W. Pritzkow, *Isotope Dilution Mass Spectrometry – A primary method of measurement and its role for RM certification*, MAPAN, 2009, submitted.
129 C. Brunnée, H. Voshage, "*Massenspektrometrie*"; Verlag K. Thiemig, Munich, 1964.
130 P. J. Turner, D. J. Mills, E. Schröder, G. Lapitajs, G. Jung, L. A. Iacone, D. A. Haydar, A. Montaser, Basic Concepts of High Resolution ICPMS, in: Montaser, *Inductively Coupled Plasma Mass Spectrometry*, Wiley-VCH, New York (1998) S. 446–459.
131 A. Benninghoven, F. G. Rudenauer, and H. W. Werner, *Secondary Ion Mass Spectrometry: Basic Concepts, Instrumental Aspects, Applications and Trends*; John Wiley and Sons, New York, 1987.
132 D. Ardelt and U. Heyen, *First results with a new multichannel ion detector. Talk W05 at the 2010 Winter Conference on Plasma Spectrochemistry*, January 4–9, 2010, Fort Myers, Florida.
133 F. F. Chen, *Introduction to Plasma Physics*, Plenum Press, New York, 1974.
134 R. Payling, D. Jones, and A. Bengtson (ed.), *Glow Discharge Optical Emission Spectrometry*, John Wiley & Sons, Chichester, 1997.
135 R. K. Marcus and J. A. C. Broekaert (ed.), *Glow Discharge Plasmas in Analytical Spectroscopy*, John Wiley & Sons, Chichester, 2003.
136 V. Hoffmann, M. Kazik, P. Robinson and C. Venzago, *Anal. Bioanal. Chem.*, 2005, **381**, 173–188.
137 M. R. Winchester and R. Payling, *Spectrochim. Acta, Part B*, 2004, **59**, 607–666.
138 G. D. Schilling, F. J. Andrade, J. H. Barnes IV, R. P. Sperline, M. B. Denton, C. J. Barinaga, D. W. Koppenaal and G. M. Hieftje, *Anal. Chem.*, 2007, **79**, 7662–7668.
139 For more details see Brochure Finnigan Tm Element GD Glow Discharge Mass Spectrometer, Thermo Electron Cooperation, 2005. homepage of Thermo Fisher Scientific.
140 M. Hamester, L. Rottmann and J. Hinrichs, *Labor Praxis, Jan./Febr*, 2006, 42–44.
141 C. B. Douthitt, *Anal. Bioanal. Chem.*, 2008, **390**, 437–440.
142 S. F. Boulyga, U. Klötzli and T. Prohaska, *J. Anal. At. Spectrom.*, 2006, **21**, 1427–1430.
143 D. Ardelt, U. Heyen, *First results with a new multichannel ion detector. Talk W05 at the 2010 Winter Conference on Plasma Spectrochemistry*, January 4–9, 2010, *Fort Myers, Florida*.
144 http://www.spectro.com/pages/e/p060124_New_Era_in_ICP_Mass_Spectrometry.htm.
145 F. Vanhaecke, L. Moens and R. Dams, *J. Anal. At. Spectrom.*, 1998, **13**, 1189–1192.
146 M. Morita, H. Ito, M. Linscheid and K. Otsuka, *Anal. Chem.*, 1994, **66**, 1588–1590.
147 F. Vanhaecke, L. Balcaen and D. Malinovsky, *J. Anal. At. Spectrom.*, 2009, **24**, 863–886.
148 S. Weyer and J. Schwieters, *Int. J. Mass Spectrom.*, 2003, **226**, 355–368.
149 K. G. Heumann, S. M. Gallus, G. Rädlinger and J. Vogl, *J. Anal. At. Spectrom.*, 1998, **13**, 1001–1008.
150 C. Quetel, J. Vogl, T. Prohaska, S. Nelms, P. Taylor and P. De Bièvre, *Fresenius J. Anal. Chem.*, 2000, **368**, 148–155.
151 S. Swoboda, M. Brunner, S. Boulyga, P. Galler, M. Horacek and T. Prohaska, *Anal. Bioanal. Chem.*, 2008, **390**, 487–494.
152 T. Prohaska, C. Latkoczy, G. Schultheis, M. Teschler-Nicola and G. Stingeder, *J. Anal. At. Spectrom.*, 2002, **17**, 887–891.
153 P. Galler, A. Limbeck, S. F. Boulyga, G. Stingeder, T. Hirata and T. Prohaska, *Anal. Chem.*, 2007, **79**, 5023–5029.
154 F. Vanhaecke and L. Moens, *Anal. Bioanal. Chem.*, 2004, **378**, 232–240.
155 J. R. de Laeter, J. K. Böhlke, P. De Bièvre, H. Hidaka, H. S. Peiser, K. J. R. Rosman and P. D. P. Taylor, *Pure Appl. Chem.*, 2003, **75**, 683–800.
156 T. Prohaska, C. R. Quetel, C. Hennessy, D. Liesegang, I. Papadakis, P. D. P. Taylor, C. Latkoczy, S. Hann and G. Stingeder, *J. Environ. Monit.*, 2000, **2**, 613–620.
157 F. Faure and T. M. Mensing, in *Isotopes, principles and applications*, Wiley, New Jersey, 3rd edn, 2005, p. 78.
158 C. P. Ingle, B. L. Sharp, M. S. A. Horstwood, R. R. Parrish and D. J. Lewis, *J. Anal. At. Spectrom.*, 2003, **18**, 219–229.
159 L. Yang and R. Sturgeon, *J. Anal. At. Spectrom.*, 2003, **18**, 1452–1457.
160 C. Cloquet, Ph.D. Thesis, CRPG-CNRS, France, 2005.
161 J. K. Böhlke, J. R. de Laeter, P. De Bièvre, H. Hidaka, H. S. Peiser, K. J. R. Rosman and P. D. P. Taylor, *J. Phys. Chem. Ref. Data*, 2005, **34**, 57–67.
162 T. Ohno and T. Hirata, *Anal. Sci.*, 2007, **23**, 1275–1280.
163 L. Moens, F. F. Vanhaecke, D. R. Bandura, V. I. Baranov and S. D. Tanner, *J. Anal. At. Spectrom.*, 2001, **16**, 991–994.
164 A. Rowland, T. B. Housh and J. A. Holcombe, *J. Anal. At. Spectrom.*, 2008, **23**, 167–172.
165 P. Cheng, G. K. Koyanagi and D. K. Bohme, *Anal. Chim. Acta*, 2008, **627**, 148–153.
166 T. Ohno and T. Hirata, *Anal. Sci.*, 2007, **23**, 1275–1280.
167 T. Ohno, T. Komiya, Y. Ueno, T. Hirata and S. Maruyama, *Gondwana Res.*, 2008, **14**, 126–133.
168 M. E. Ketterer, M. J. Peters and P. J. Tisdale, *J. Anal. At. Spectrom.*, 1991, **6**, 439–443.
169 D. S. Lauretta, B. Klaue, J. D. Blum and P. R. Buseck, *Geochim. Cosmochim. Acta*, 2001, **65**, 2807–2818.
170 J. D. Blum, A. Bridget and A. Bergquist, *Anal. Bioanal. Chem.*, 2007, **388**, 353–359.
171 A. J. Pietruszka, R. J. Walker and P. A. Candela, *Chem. Geol.*, 2006, **225**, 121–136.

172 F. Wombacher and M. Rehkaemper, *J. Anal. At. Spectrom.*, 2003, **18**, 1371–1375.
173 J. Woodhead, *J. Anal. At. Spectrom.*, 2002, **17**, 1381–1385.
174 G. P. Russ III, *Applications of Inductively Coupled Plasma MassSpectrometry*, ed. A. R. Date and A. L. Gray, Blackie, Glasgow, 1989, 4, 90–114.
175 S. M. Nelms, C. R. Quetel, T. Prohaska, J. Vogl and P. D. P. Taylor, *J. Anal. At. Spectrom.*, 2001, **16**, 333–338.
176 Perkin Elmer, Elan 6100 DRC Software guide for software version 2.3.2, May 2000.
177 F. Vanhaecke, G. de Wannemacker, L. Moens, R. Dams, C. Latkoczy, T. Prohaska and G. Stingeder, *J. Anal. At. Spectrom.*, 1998, **13**, 567–571.
178 E. A. Kurz, *Am. Lab.*, 1979, 67–82.
179 L. A. Dietz, *Rev. Sci. Instrum.*, 1965, **36**, 1763–1770.
180 G. P. Russ and J. M. Bazan, *Spectrochim. Acta, Part B*, 1987, **42**, 49–62.
181 M. E. Wieser and J. B. Schwieters, *Int. J. Mass Spectrom.*, 2005, **242**, 97–115.
182 N. Jakubowski, T. Prohaska, F. Vanhaecke, P. H. Roos and T. Lindemann, *J. Anal. At. Spectrom.*, 2011, **26**, DOI: 10.1039/c0ja00007h.

